

The roles of two *C. elegans* HOX co-factor orthologs in cell migration and vulva development

Lucie Yang*, Mary Sym† and Cynthia Kenyon§

Department of Biochemistry and Biophysics, University of California, San Francisco, Mission Bay Genentech Hall, 600 16th Street, Room S312A, San Francisco, CA 94143-2200, USA

*Present address: Department of Surgery, University of California, San Francisco CA 94143, USA

†Present address: Carolina Center for Genome Sciences, University of North Carolina at Chapel Hill, Chapel Hill, NC 27599-7264, USA

§Author for correspondence (e-mail: ckenyon@biochem.ucsf.edu)

Accepted 26 October 2004

Development 132, 1413-1428
Published by The Company of Biologists 2005
doi:10.1242/dev.01569

Summary

Anteroposterior cell migration and patterning in *C. elegans* are governed by multiple, interacting signaling pathways and transcription factors. In this study, we have investigated the role of *ceh-20*, the *C. elegans* ortholog of the HOX co-factor Extradenticle (Exd/Pbx), and *unc-62*, the *C. elegans* ortholog of Homothorax (Hth/Meis/Prep), in two processes that are regulated by Hox gene *lin-39*: cell migration and vulva formation. As in *lin-39* mutants, the anterior migrations of neuroblasts in the Q lineage are truncated in Hox co-factor mutants. Surprisingly, though, our findings suggested that the roles of *ceh-20* and *unc-62* are different from that of *lin-39*; specifically, *ceh-20* and

unc-62 but not *lin-39* are required for the transmembrane protein MIG-13 to promote anterior migration. To our knowledge, *ceh-20* and *unc-62* are the only genes that have been implicated in the *mig-13* pathway. We find that *ceh-20* and *unc-62* are also required for several steps in vulva development. Surprisingly, *ceh-20* and *unc-62* mutants have phenotypes that are starkly different from those of *lin-39* mutants. Thus, in this process, too, *ceh-20* and *unc-62* are likely to have functions that are independent of *lin-39*.

Key words: Hox co-factor, *ceh-20*, *unc-62*, Cell migration, Vulva development, *C. elegans*

Introduction

In *Caenorhabditis elegans*, Hox genes specify patterns of cell migration, cell division, differentiation and morphogenesis along the anteroposterior body axis. In this study, we have characterized mutations in two genes: *ceh-20*, which encodes the *C. elegans* ortholog of the Hox co-factor Extradenticle (Exd/Pbx); and *unc-62*, which encodes the *C. elegans* ortholog of the Hox co-factor Homothorax (Hth/Meis/Prep). Like Hox mutations, mutations in these co-factors influence multiple cell-fate decisions. In this study, we have analyzed the effects of these mutations on two different processes, Q neuroblast migration and vulva development, both of which are known to be influenced by the *C. elegans* Hox gene *lin-39*.

The *C. elegans* Q neuroblasts, QL and QR, and their descendants migrate long distances along the anteroposterior body axis. QL and QR are born as bilaterally symmetric cells in the posterior body region of the animal (Fig. 1A) (Chalfie and Sulston, 1981; Sulston and Horvitz, 1977). The right Q cell (QR) and its descendants migrate towards the anterior, whereas the left Q cell (QL) and its descendants migrate towards the posterior. The stopping points of the Q descendants are not associated with any obvious landmarks, and the mechanisms by which their final positions are specified are not well understood.

Several genes are known to influence these stopping points, including *lin-39*, *mig-13* and *egl-20*. *lin-39* is a Hox gene, the *C. elegans* ortholog of the *Drosophila* homeobox genes *Sex combs reduced/Deformed/proboscidia* (Clark et al., 1993; Wang et

al., 1993). *lin-39* is expressed in QR and its descendants and acts cell autonomously to promote the anterior migration of these cells (Clark et al., 1993; Wang et al., 1993). *mig-13* encodes a novel transmembrane protein (Sym et al., 1999). This protein acts extrinsically of the Q descendants to promote their anterior migration in a dose-dependent manner, in which progressively higher protein levels, even if delivered throughout the body, promote progressively further anterior migration (Sym et al., 1999). In addition, increasing MIG-13 levels can cause cells that normally migrate posteriorly to stop migrating prematurely or reverse direction and migrate anteriorly. *egl-20* encodes a Wnt protein (Maloof et al., 1999; Whangbo and Kenyon, 1999). Like *mig-13*, *egl-20* is required to promote anterior migration of the QR descendants. Although *egl-20* is expressed in the tail, ectopic or global *egl-20* expression can restore full anterior migrations of QR descendants in animals with reduced *egl-20* activity. Genetic and molecular experiments suggest that *lin-39*, *mig-13* and *egl-20* act in partially independent pathways to regulate the anterior migrations of the QR descendants (Harris et al., 1996; Sym et al., 1999).

The *egl-20* gene also influences the migrations of cells in the QL lineage, but in a different way. In QL, EGL-20 switches on expression of the Hox gene *mab-5*, the *C. elegans* ortholog of *Drosophila Antennapedia*, via a canonical Wnt signaling pathway. *mab-5* acts cell-autonomously in the QL lineage, and is necessary and sufficient to promote the posterior migrations of QL descendants (Harris et al., 1996; Salser and Kenyon, 1992).

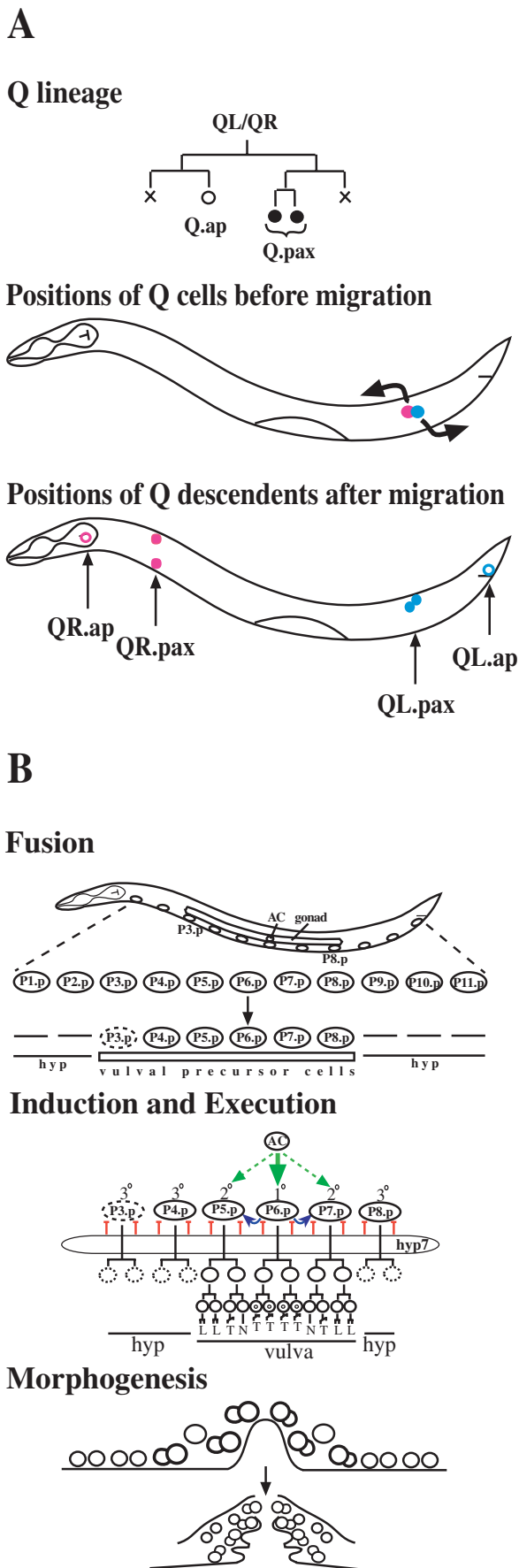


Fig. 1. (A) Wild-type Q lineage and cell migration. (Top) Q neuroblast lineage. QL and QR generate identical cell lineages to produce three neurons: the two Q.pax cells are filled circles whereas the Q.ap cell is an unfilled circle. 'X' indicates cell death. (Middle) Left and right Q cells (QL in blue, QR in pink) are located in approximately the same position at hatching. Anterior is towards the left and ventral is downwards. Shortly after hatching but before division, the QL cell migrates a short distance posteriorly, while the QR cell migrates a short distance anteriorly. (Bottom) Final positions of Q descendants. QL.pax cells (filled blue circles) are located near the position of QL at hatching, whereas the QL.ap (unfilled blue circle) cell migrates into the tail. QR.pax cells (filled pink circles) migrate to the anterior body, whereas the QR.ap cell (unfilled pink circle) migrates into the head. (B) Wild-type vulva development. (Top) A schematic view of a late L1 larva with 11 of the 12 ventral Pn.p cells shown. Some of the Pn.p cells fuse with the hypodermal syncytium, hyp7, as indicated by dashes in the third row of the top panel. The unfused cells are indicated by ovals, and these are the vulval precursor cells (VPCs). The oval around P3.p is dashed because this cell remains unfused in about 50% of wild-type animals. Anterior is towards the left and ventral is downwards. (Middle) In the L3 stage, an inductive signal (green arrows) from the anchor cell (AC, also shown in the top panel), lateral signaling (blue arrow) among the VPCs and an inhibitory signal (red T) from hyp7 impose a 3° - 3° - 2° - 1° - 2° - 3° pattern of cell fates. The three fates can be distinguished by the expression pattern of several markers and by cell lineage pattern. The 1° fate is characterized by three rounds of cell division, with the last divisions being all transverse (T). The 2° fate is characterized by three rounds of cell division, with the Pn.pxx cells dividing longitudinally (L), dividing transversely (T) or not dividing (N). The 3° fate is characterized by a single round of division followed by fusion with hyp7, as indicated by the dashed Pn.px circles. The descendants of P5.p-P7.p form the vulva. (Bottom) In the L4 stage, the vulval cells migrate towards the center of the animal to form seven vulval rings and begin the process of intratoroidal fusion. Vulval eversion at the end of the vulva formation process is not shown.

In addition to regulating neuroblast migration, the Hox gene *lin-39* also regulates vulva development. The vulva is generated by a subset of the 12 ventral epidermal cells that are located in a row along the ventral margin of the animal (Fig. 1B) (for reviews, see Greenwald, 1997; Shemer and Podbilewicz, 2003; Wang and Sternberg, 2001). These cells, called P(1-12).p, are born during the first larval stage. Soon after their birth, all but the six central Pn.p cells, P(3-8).p, fuse with the epidermal syncytium, hyp7 (Sulston and Horvitz, 1977). P(3-8).p are prevented from undergoing cell fusion by LIN-39. CEH-20 also participates in cell fusion (Shemer and Podbilewicz, 2002). Together with LIN-39, CEH-20 represses *eff-1*, a gene required for cell fusion (Mohler et al., 2002; Shemer and Podbilewicz, 2002). CEH-20 and LIN-39 also regulate the activity of *egl-18* and *elt-6*, GATA factors that redundantly inhibit cell fusion (Koh et al., 2002). Furthermore, all of the Pn.p cells fused with hyp7 in most *ceh-20(ay42)* animals (Shemer and Podbilewicz, 2002).

During the L3 stage, three of the six vulval precursor cells (VPCs), P(5-7).p, are induced by the nearby gonadal anchor cell to generate the vulval cell lineages. The other VPCs, P(3,4, and 8).p, divide once, and their daughters then fuse with hyp7. Vulval cell-lineage specification is controlled by several interacting signaling pathways. The 'synMuv' pathway plays an important role in determining whether a Pn.p cell generates

vulval cell lineages or not. This pathway prevents vulval cell division in the absence of an inductive signal from the anchor cell (reviewed by Fay and Han, 2000). Animals defective in both class A and class B synMuv gene functions display a multivulval phenotype because most of the vulval precursor cells adopt vulval fates (Ferguson and Horvitz, 1989). Many of the synMuv pathway components are members of the nucleosome remodeling and histone deacetylation (NuRD) complex or proteins that physically interact with histone deacetylases (Brehm et al., 1998; Lu and Horvitz, 1998; Solari and Ahringer, 2000). By antagonizing the Ras pathway, the NuRD complex helps to limit the number of cells adopting vulval fates.

Other signaling pathways involved in vulval lineage specification include: (1) the Ras, Wnt and Rb pathways, and the SEM-4 transcription factor, which upregulate *lin-39* expression and allow the three Pn.p cells located closest to the anchor cell to overcome the silencing effects of the synMuv genes and generate vulval cell lineages (Chen and Han, 2001a; Eisenmann et al., 1998; Grant et al., 2000; Hoier et al., 2000; Maloof and Kenyon, 1998); (2) the Hox gene *lin-39*, which upregulates its own expression to permit vulval induction and to instruct cells to generate vulval cell types instead of different, posterior-specific, cell types (Clandinin et al., 1997; Clark et al., 1993; Maloof and Kenyon, 1998; Wang et al., 1993); and (3) the forkhead-family transcription factor LIN-31, which prevents a randomization of lineage patterns (Tan et al., 1998). Once the 22 vulval cells have been generated, they undergo a complex pattern of vulval morphogenesis which includes the migration of P5.p and P7.p descendants towards the descendants of P6.p during the final stages of postembryonic development.

In this study, we show that the *C. elegans* Hox co-factor orthologs *ceh-20* and *unc-62* are required for two processes that are also regulated by Hox gene *lin-39*: (1) anterior migration of the QR neuroblast and its descendants; and (2) vulva formation. Surprisingly, we find that *ceh-20* and *unc-62*, but not *lin-39*, are required for MIG-13 to promote anterior migration. To our knowledge, *ceh-20* and *unc-62* are the only two genes that have been implicated to function with *mig-13* in regulating anterior migration. We also find that *ceh-20* and *unc-62* are required for several steps in vulva formation, and mutations in these genes result in phenotypes that are starkly different from those previously shown for *lin-39* mutants. Thus, in both processes, these Hox co-factor orthologs may function, in part, independently of the Hox gene *lin-39*.

Materials and methods

Genetics and phenotypic analysis

Standard methods for culturing and genetic analysis were used (Brenner, 1974; Sulston and Hodgkin, 1988). Strains were maintained at 20°C. Strains used in this study are:

N2 wild-type var. Bristol,
tax-4::gfp,
mig-13(mu225) X; *tax-4::gfp*,
ceh-20(mu290) III; *tax-4::gfp*,
unc-62(mu232) V; *tax-4::gfp*,
mab-5(e2088) III; *tax-4::gfp*,
lin-39(n1760) III; *tax-4::gfp*,
ceh-20(mu290) III,
ceh-20(mu290) III; *muls32[mec-7::gfp] II*,

unc-62(mu232) V,
unc-62(mu232) V; *muls32[mec-7::gfp] II*,
unc-62(ku234) V,
unc-62(s472) V unc-46(e177);yDp1(IV;V;f),
mig-13(mu225) X, *lin-39(n1760) III*,
ceh-20(mu290) lin-39(n1760) III,
unc-62(mu232) V; *lin-39(n1760) III*,
mab-5(e2088) III,
ceh-20(mu290) mab-5(e2088) III,
unc-62(mu232) V; *mab-5(e2088) III*,
mig-13(mu31) X,
mig-13(mu225) X,
egl-20(n585) IV,
mig-13(mu31) X; *egl-20(n585) IV*,
egl-20(mu320) IV,
ceh-20(mu290) III; *egl-20(mu320) IV*,
ceh-20(mu290) III; *egl-20(n585) IV*,
ceh-20(mu290) III; *mig-13(mu31) X*,
unc-62(mu232) V; *egl-20(mu320) IV*,
unc-62(mu232) V; *egl-20(n585) IV*,
unc-62(mu232) V; *mig-13(mu31) X*,
lin-39(n1760) III; *egl-20(mu320) IV*,
lin-39(mu26) III; *mig-13(mu31) X*,
muEx89 [Punc-119::mig-13GFP],
mig-13(mu225) X; *muEx89 [Punc-119::mig-13GFP]*,
lin-39(n1760) III; *muEx89 [Punc-119::mig-13GFP]*,
ceh-20(mu290) III; *muEx89 [Punc-119::mig-13GFP]*,
unc-62(mu232) V; *muEx89 [Punc-119::mig-13GFP]*,
ceh-20(mu290) III; *muEx261 [ceh-20::gfp + odr-1::rfp]*,
rrf-3(pk1426); *muls35 [mec-7::gfp]*,
nDf16/qC1[dyp-19(e1259) glp-1(q339)] III,
unc-62(s472) unc-46(e177) V; *yDp1(IV;V;f)*,
wIs52[scm::gfp::lac-Z; unc-119(+)] (Koh and Rothman, 2001),
ceh-20(mu290) III; *wIs52[scm::gfp::lac-Z; unc-119(+)]*,
unc-62(mu232) V; *wIs52[scm::gfp::lac-Z; unc-119(+)]*,
jcIs1[jam-1::gfp; rol-6(d)] (Mohler et al., 1998),
ceh-20(mu290) III; *jcIs1[jam-1::gfp; rol-6(d)]*,
unc-62(mu232) V; *jcIs1[jam-1::gfp; rol-6(d)]*,
ceh-20(mu290) III; *ayIs9[egl-17::gfp]*,
mu232; *ayIs9[egl-17::gfp]*,
muls3[mab-5::lacZ, rol-6(d)],
ceh-20(mu290) III; *muls3[mab-5::lacZ, rol-6(d)]*,
unc-62(mu232); *muls3[mab-5::lacZ, rol-6(d)]*,
ceh-20(mu290) III; *unc-62(mu232) V*

The positions of the Q.pa daughters were determined directly using Nomarski optics at the end of L1. At this stage, the hypodermal V cells have divided once and the P nuclei have all descended into the cord. The positions of the Q.pa daughters were scored relative to the V cell daughters. The Q.ap cell positions were determined using an integrated *tax-4::GFP* fusion (Sym et al., 1999). Cell positions of Q descendants were analyzed only in animals without additional neurons in the body. In principle, this could introduce a selection bias; however, we addressed this by extensive lineage analysis and other methods (see Fig. S1 in the supplementary material). If the cell(s) of interest migrated near a Vn.a cell that had divided, the 'Vn.a position' was defined as the distance bounded by a dorsoventral line through the center of the Vn.aa nucleolus and a dorsoventral line through the center of the Vn.ap nucleolus. Statistical analyses on the QR.pax distributions were performed using the Mann-Whitney test on AVM and SDQR separately.

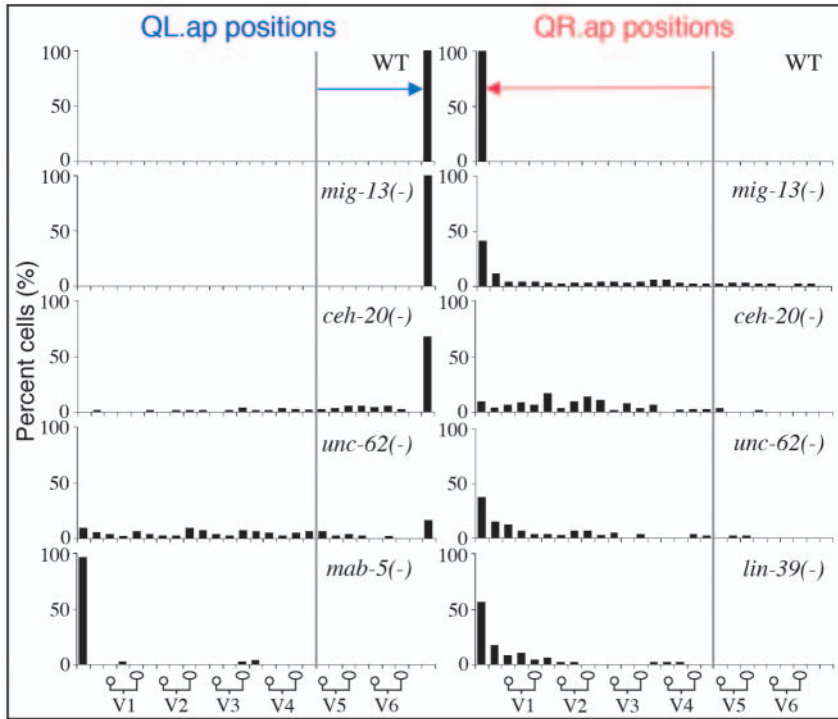


Fig. 2. Cell migration defects in *che-20(-)* and *unc-62(-)* mutants. The final positions of the QL.ap (left column) and QR.ap (right column) cells are graphed using the V cell daughters as reference points along the *x* axis, with left being anterior. The QL.ap cells in *che-20(mu290)* and *unc-62(mu232)* can be displaced anterior to the wild-type (WT) and *mig-13(mu31)* positions, but not as far anteriorly as in *mab-5(e2088)* animals. The QR.ap positions in *che-20(mu290)* and *unc-62(mu232)*, as in *mig-13(mu31)* and *lin-39(n1760)* (although to a lesser degree in the latter), are significantly posterior to those found in wild type. The vertical gray line indicates the birthplace of the Q cells. The blue arrow indicates the total posterior distance that QL, QL.a and QL.ap migrate in wild-type animals. The pink arrow indicates the total anterior distance that QR, QR.a and QR.ap migrate in wild-type animals. $n \geq 100$ cells for each strain.

che-20 mutant isolation and characterization

The *mu290* mutation was identified in a Nomarski screen for mutants with misplaced Q.ap cells in mutagenized *tax-4::gfp* animals. Mutants were generated with ethyl methanesulfonate (EMS). The QR.pax cell positioning defect was assayed in mapping experiments. *mu290* was mapped using STS mapping (Williams et al., 1992) to a 0.7 map unit region tightly linked to the physical marker *stP120* at the center of LG III. Chromosomal deficiencies were then used to refine the map position. The QR.pax positioning defect was generated when *mu290* was placed in trans to the deficiency *nDf16*. Transformation rescue of the QR.pax cell positioning phenotype was obtained with pools of cosmids in this region. Ultimately, the rescuing activity of the QR.pax cell positioning defect, as well as the multivulval and egg-laying defects, were obtained with a single cosmid, F31E3. This cosmid also rescued the extra ventral protrusion phenotype of mutant hermaphrodites. A candidate open reading frame for *mu290* was F31E3.1, which encodes a *C. elegans* ortholog of Exd/Pbx (Burglin and Ruvkun, 1992). A 3.6 kb PCR fragment that encompasses this gene was injected at 1 ng/ μ l with pPD93.97 (*myo-3::gfp*) at 100 ng/ μ l into *mu290* animals. Four out of four lines generated with this PCR fragment gave 48–75% rescue of the QR.pax defect and over 85% rescue of the vulval defect. To identify the molecular lesion in *che-20(mu290)*, we isolated and sequenced cDNA clones generated by RT-PCR (Frohman, 1993) from wild-type and *che-20(mu290)* DNA. The oligo(dT) primer was used to obtain the 3' end and the spliced leader sequence SL1 primer to obtain the 5' cDNA end. Only a single

isoform was isolated from several clones. A single G to A transition was identified in the cDNA product derived from *che-20(mu290)*. This mutation changes a conserved arginine (R) in the 3rd helix of the homeodomain to a histidine. This R has been implicated as part of a nuclear localization signal (NLS) in the third helix of the homeodomain that is less conserved than the classical NLS RRKRR found at the N-terminal arm of the homeodomain. The R that is mutated in *che-20(mu290)* is the second R in this less conserved and weaker NLS, KRIRYKKN (Abu-Shaar et al., 1999; Saleh et al., 2000a). *che-20(mu290)/qC1[dyp-19(e1259) glp-1(q339) III; him-5(e1490)* was used for crosses since it was very difficult to mate into *che-20(mu290)*. Animals were outcrossed at least three times before phenotypes were studied.

unc-62 mutant isolation and characterization

The *mu232* mutation was identified in a screen for mutants with misplaced Q.pax cells in mutagenized *mec-7::gfp* animals, as described by Ch'ng et al. (Ch'ng et al., 2003). In *mu232/+* animals, the QR.pax cells were in wild-type positions, indicating that *mu232* is recessive and thus likely to be a reduction or loss-of-function allele. We mapped *mu232* to chromosome VL near *stP3* and *unc-62*. *mu232* failed to complement *s472*, a null *unc-62* allele, for the QR.pax cell-positioning defect, suggesting that *mu232* is an allele of *unc-62*. *mu232/s472* animals have a stronger QR.pax phenotype than *mu232* animals, consistent with *mu232* being a hypomorph. *unc-62* exons were amplified from wild-type and *mu232* using primers around each predicted exon. Sequencing these genomic fragments revealed that *mu232* harbored a T→A transition that changed the predicted initial Met(ATG) codon of exon 1b to a Lys(AAG) codon. We also sequenced *unc-62(ku234)* (Van Auken et al., 2002) and discovered a G→A transition in the same codon. *mu232* failed to complement *ku234* (gift from Meera Sundaram) for the QR.pax positioning and Egl phenotypes. Because *mu232* and *ku234* exhibited the lowest percentage of embryonic and larval lethality among the known *unc-62* homozygous alleles, we examined larval phenotypes using *mu232* after noting that *mu232* and *ku234* exhibit very similar migration and vulval phenotypes. *mu232* was outcrossed more than three times before phenotypes were studied.

Ectopic expression of *mig-13*

After verifying that the extrachromosomal array, *muEx89(P_{unc-119}::mig-13GFP)* (Q. Ch'ng, PhD thesis, University of California, 2001), could create an anterior-promoting environment mimicking that created by *hs-mig-13* [see Fig. 5 for rescued positions of QR.pax and BDU in *mig-13(-)*], we crossed *muEx89* into *che-20(mu290)*, *unc-62(mu232)*, and *lin-39(n1760)*. In animals that were green, we believe that *mig-13::GFP* was ectopically expressed because ALM (data not shown) and CAN (see Fig. S4 in the supplementary material) were redirected to more anterior positions.

che-20::GFP expression

A translational *che-20::GFP* fusion was constructed by inserting the GFP coding region of pPD119.45 into an *AgeI* site engineered just 5' to the last stop codon of *che-20*. Transgenic arrays were generated using standard techniques (Mello et al., 1991). The resulting plasmid (pLY11) was injected at 50 ng/ μ l with *odr-1::rfp* (generously provided by Cori Bargmann's laboratory) at 100 ng/ μ l into *che-*

20(*mu290*) hermaphrodites. Several transgenic lines rescuing the QR.pax defect and the *muv* defect were established, and all showed similar expression patterns. The line used in this study was *muEx261*.

Immunofluorescence and β -galactosidase detection

LIN-39 antibody staining was performed as described by Maloof and Kenyon (Maloof and Kenyon, 1998). Staged populations of animals were stained with both the LIN-39 antibody and the monoclonal antibody MH27 (Francis and Waterston, 1991). Individual slides with animals of different genotypes were stained simultaneously under identical conditions prior to comparison, and the differences in staining intensity were repeatable. For *mab-5* expression, staged populations of *mulS3[mab-5::lacZ, rol-6(d)]*, *ceh-20(mu290); mulS3[mab-5::lacZ, rol-6(d)]*, and *unc-62(mu232); mulS3[mab-5::lacZ, rol-6(d)]* animals were grown at 20°C. Larvae were fixed on slides and stained as described by Maloof et al. (Maloof et al., 1999).

Lineage analysis and microscopy

Analysis of Q lineages and Vn.a lineages were performed from hatching to late L1/early L2. Of the 27 wild-type Q cells whose lineages were analyzed, Q.pp and Q.aa were still present by late L1/early L2 in only four (14.8%) and three animals (11.1%), respectively, and none of the Q cell descendants divided inappropriately. Vulval lineages were observed starting with the Pn.px cell stage until the L4 molt by Nomarski optics.

RNA interference

rrf-3(pk1426) is more sensitive than wild-type animals to RNAi (Simmer et al., 2002). *rrf-3(pk1426); mulS35[mec-7::gfp]* animals in L4 were grown on bacteria containing vector only or on bacteria expressing *ceh-20* dsRNA, *unc-62* dsRNA or *lin-39* dsRNA. Their progeny were analyzed for QR.pax positions in late L1, vulval induction in L4, and number of ventral protrusions as young adults. Animals fed with the control plasmid did not display the QR.pax positioning defect, vulval induction defects or additional ventral protrusions.

Characterization of vulval phenotypes

Pn.p cell fusion status was scored by first crossing *jam-1::gfp* (Mohler et al., 1998) into *ceh-20(mu290)* and *unc-62(mu232)*. The early L1 fusion event was scored in L2 when the adherens junctions of unfused cells were visible as a circle. The later fusion event was scored in L3.

Vulval induction was scored at the L4 stage under Nomarski optics (Sternberg and Horvitz, 1986). Nuclei that were not hypodermal, neuronal or muscle were counted. The number of vulval nuclei was used to extrapolate the number of induced Pn.p cells. A Pn.p cell in which both daughter cells divide one more time, and both granddaughters divide to generate seven or eight great granddaughters and no hypodermal tissue was scored as 1.0 cell induction. A Pn.p, which generates more than two but fewer than seven or eight cells was scored as 0.5 cell induction. In wild-type, P5.p, P6.p and P7.p each undergo a 1.0 cell induction whereas the other Pn.p cells are not induced, resulting in a total cell induction of 3.0.

Results

ceh-20 encodes an *extradenticle*-like gene required for Q-descendant migration

In the wild-type, the Q.ap cells migrate either towards the head (QR lineage) or tail (QL lineage). We isolated the mutation *mu290* (see Materials and methods) in a screen for mutants with improperly positioned Q.ap cells using a *tax-4::GFP* fusion, which is expressed in the Q.ap cells. Subsequent genetic and molecular analyses indicated that *mu290* is an

allele of the Hox co-factor *ceh-20* (see Materials and methods). The molecular lesion in *ceh-20(mu290)* is a G→A transition that alters a conserved arginine to histidine in a nuclear localization signal consensus site in the third helix of the homeodomain (Abu-Shaar et al., 1999; Passner et al., 1999; Piper et al., 1999; Saleh et al., 2000a).

In ~90% of *ceh-20(mu290)* animals, QR.ap was located between the birthplace of QR and its wild-type location in the head (Fig. 2). In addition, the QR.pax cells were in the central body region rather than in the anterior (Fig. 3), suggesting that cells in the QR lineage stopped migrating prematurely. In ~33% of *ceh-20(mu290)* animals, QL.ap was not located in its normal position in the tail (Fig. 2). In fact, QL.ap could be found anterior to the birthplace of QL in ~10% of *ceh-20* mutants, suggesting that this cell had migrated anteriorly instead of posteriorly.

Unexpectedly, we also found additional neuronal cells in the mid-body region (~25% on both left and right sides). By observing the sequence of Q cell divisions using Nomarski optics, we found that these cells resulted from inappropriate cell survival and division in the Q cell lineages. In wild-type animals, Q.pp and Q.aa die by apoptosis, and most of these cells disappear by the end of L1. Of the 27 wild-type Q cells lineaged to the end of L1, only four Q.pp and three Q.aa cells remained visible, and none of the Q cell descendants divided inappropriately. However, in nine of the 20 *ceh-20(mu290)* animals we analyzed, Q.pp remained visible. Furthermore, Q.pp divided in two *ceh-20* mutants and Q.ap divided in one animal.

To determine whether these phenotypes result from reduced *ceh-20* activity, we first analyzed *ceh-20(mu290)/+* heterozygotes. In *ceh-20(mu290)/+* animals, the QR.pax cells were mostly in wild-type positions (see Fig. S1 in the supplementary material) and there were no extra body neurons visible. We also found that the QR.pax phenotype was not enhanced in *ceh-20(mu290)/deficiency* heterozygotes. Finally, as RNA interference reduces gene activity, we fed *ceh-20* dsRNA to an RNAi-sensitive strain, *rrf-3* (Simmer et al., 2002). The progeny of these animals showed similar defects to those in *ceh-20(mu290)* animals, including QR.pax cells in the mid-body region and extra body neurons (see Fig. S2 in the supplementary material). Taken together, these analyses indicate that *ceh-20(mu290)* is likely to reduce gene function. Therefore, we conclude that in wild-type animals, *ceh-20* is required for the proper generation and migration of cells in the Q lineage. *ceh-20* may also have an earlier function in Q development because, in stronger alleles of *ceh-20* (obtained from M. Stern), the Q cell failed to complete its lineage (3/3 animals; data not shown).

unc-62 encodes a homothorax-like gene also required for Q descendant migration

We also screened for Q migration mutants using *mec-7::gfp*, which is expressed in QR.paa and QL.paa (Ch'ng et al., 2003). In this screen, we isolated *mu232*, a mutant with QR.pax cells located posterior to their normal stopping points (Fig. 3). Subsequent genetic and molecular analyses (Materials and methods) indicated that *mu232* is a reduction-of-function allele of the *C. elegans* homothorax (*hth*) ortholog *unc-62*, a member of the Meis family of Hox co-factors.

In *Drosophila*, *hth* and *exd* mutants have similar phenotypes.

Likewise, we found that *unc-62* mutants share the cell positioning defects exhibited by *ceh-20* mutants. In *unc-62* mutants, 70% of QR.ap cells and 100% of QR.pax cells

stopped posterior to their wild-type positions, in distributions similar to those in *ceh-20* mutants (Figs 2 and 3). Likewise, in ~70% of *unc-62* mutants, QL.ap was located anterior to the birthplace of QL (Fig. 2). Finally, QL.pax cells were in wild-type positions in *unc-62* mutants, as in *ceh-20* mutants (data not shown). The one Q phenotype that *ceh-20(mu290)* animals exhibited that *unc-62(mu232)* animals did not was the Q lineage defect.

Mutations in *ceh-20* and *unc-62* also affected the anteriorwards migration of BDU, a neuron whose cell body migrates a short distance anteriorly during embryogenesis. In ~70% of animals with a mutation in *ceh-20(mu290)* or *unc-62(mu232)*, this migration was incomplete (see below and Fig. 5).

ceh-20 and *unc-62* guide migrating cells

In theory, the shortened anterior migration of cells in mutants could simply be due to a requirement for CEH-20 and UNC-62 activity in the basic mechanisms of cell motility. However, we found that a mutation in *ceh-20* or *unc-62* could also change the direction of cell migration. First, direct observation of cell movements by Nomarski optics revealed that QR.a or QR.p migrated towards the posterior rather than the anterior direction in two out of nine *ceh-20(mu290)* animals. In addition, these *ceh-20* or *unc-62* mutations could redirect the anterior-bound cells of the QR lineage towards the posterior when combined with a mutation in a Wnt homolog *egl-20* (see below and Fig. 4). Although we cannot exclude the possibility that *ceh-20* and *unc-62* are required for some aspect of cell motility, these findings indicate that CEH-20 and UNC-62 activities are required for the guidance or positioning of cells along the AP axis.

ceh-20 and *unc-62* may promote anterior migration in a manner that does not involve the Hox gene *lin-39*

If CEH-20 and UNC-62 function as Hox co-factors like their *Drosophila* and vertebrate homologs, then *ceh-20* and *unc-62* mutants should share phenotypes with Hox mutants. Close examination of the final positions of the QR descendants in *lin-39(n1760null)*, *ceh-20(mu290)* and *unc-62(mu232)* mutants revealed that the *ceh-20* and *unc-62* mutants had a more severe cell positioning defect than did *lin-39* null animals (Fig. 3). In addition, the QR.pax cell positioning defect was more severe in the *ceh-20(mu290) lin-39(n1760)* double mutant than in either single mutant and, similarly, the *lin-39(n1760); unc-62(mu232)* double mutant phenotype was more severe than that of either single mutant (Fig. 3). Thus, CEH-20 and UNC-62 could function as LIN-39 co-factors, but they must also have a function that is independent of LIN-39 in promoting anterior migration.

ceh-20 and *unc-62*, but not *lin-39*, are required for MIG-13 to position cells along the A/P axis

QR descendants may migrate further anteriorly in *lin-39* mutants than they do in *ceh-20* or *unc-62* mutants because cells in *lin-39* mutants, but not in *ceh-20* or *unc-62* mutants, retain the ability to respond to MIG-13. Consistent with this hypothesis, the distribution of QR.pax cells in the *mig-13(mu31); lin-39(n1760)* double mutant was shifted further posteriorly than in either single mutant (data not shown) (Sym et al., 1999). This distribution nearly overlapped with the

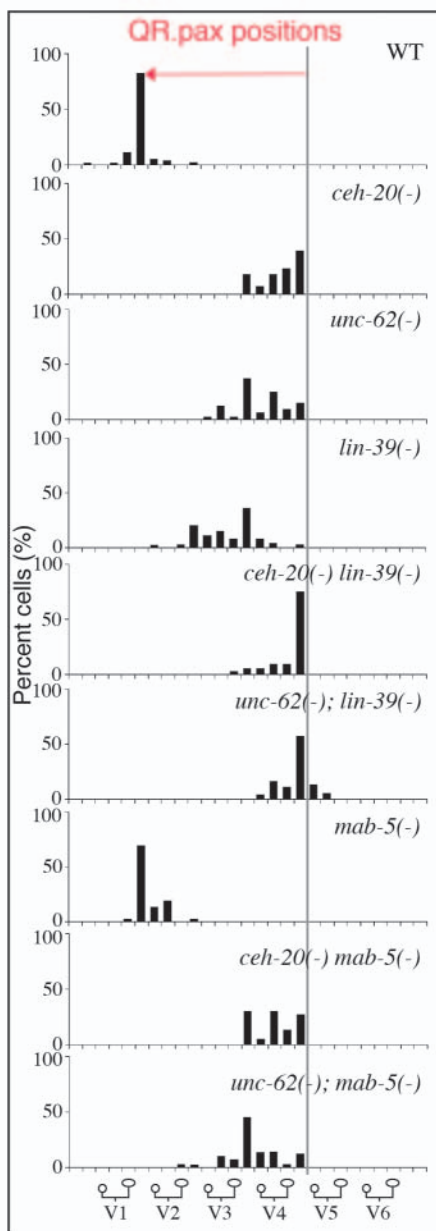


Fig. 3. *ceh-20* and *unc-62* can function independently of Hox genes *lin-39* and *mab-5* when positioning cells along the AP axis. The histograms show the distributions of QR.pax cells in wild-type animals as well as in *ceh-20(mu290)*, *unc-62(mu232)* and *lin-39(n1760)* single mutants. In the double mutants *ceh-20(mu290) lin-39(n1760)* and *unc-62(mu232); lin-39(n1760)*, the anteriorwards migrations of QR descendants are shortened. In *unc-62(mu232); lin-39(n1760)* double mutants, some cells even actively migrated towards the posterior. In the double mutants *ceh-20(mu290) mab-5(e2088)* and *unc-62(mu232); mab-5(e2088)*, QR descendants did not migrate to the wild-type positions achieved in *mab-5(e2088)* single mutants. The vertical gray line indicates the birthplace of the QR cell. The pink arrow indicates the total anterior distance traversed by QR and its descendants giving rise to QR.pax in wild-type animals. $n=100$ cells for each strain.

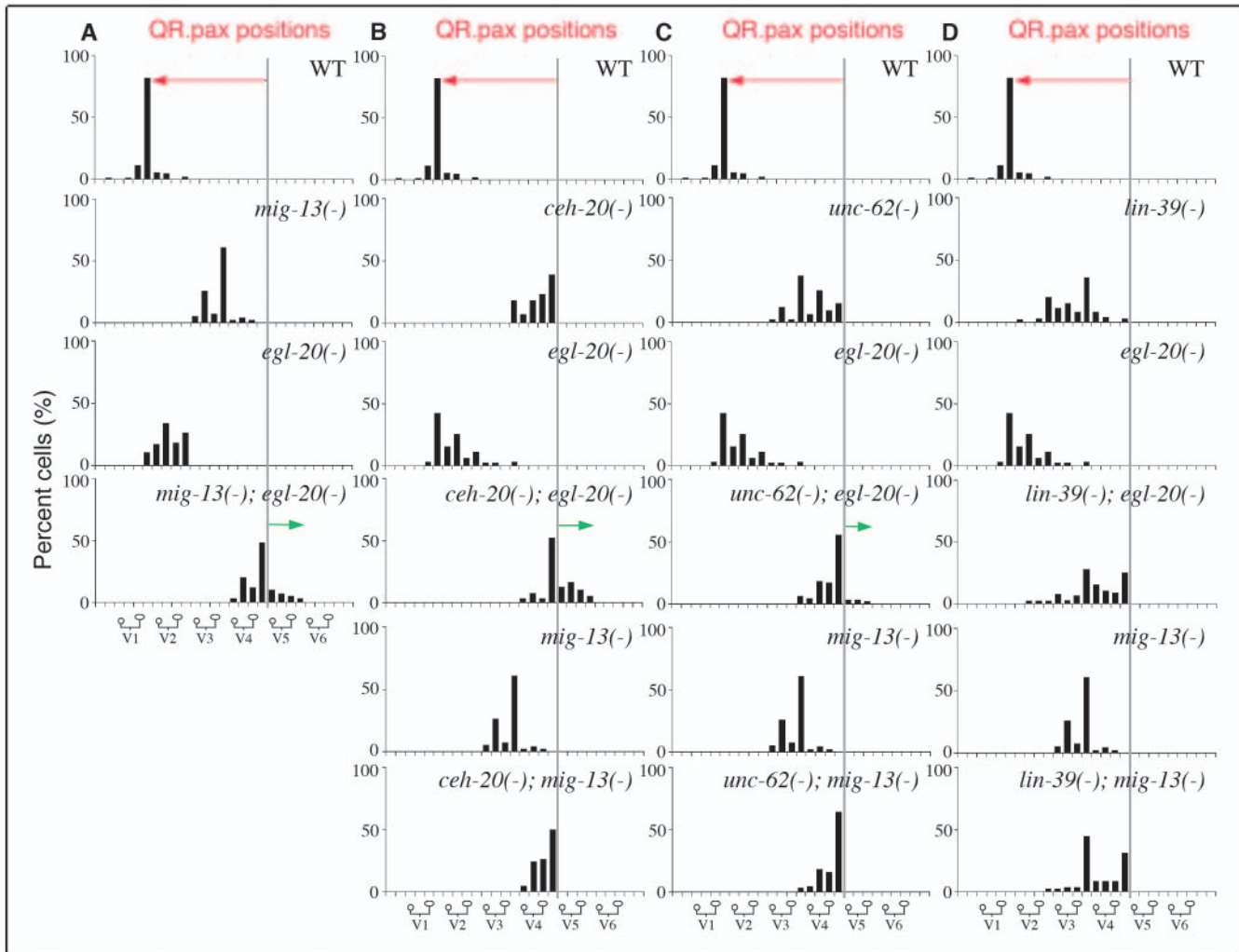


Fig. 4. *ceh-20* and *unc-62* affect cell positioning along the AP axis. (A) In the double mutant *mig-13(mu31); egl-20(n585)*, QR.pax cells were displaced further posteriorly than in *mig-13(mu31)* or *egl-20(n585)* single mutants. QR descendants actively migrated towards the posterior in many of these double mutant animals. (B,C) QR.pax cells could be displaced to a location posterior to the birthplace of QR in double mutants *ceh-20(mu290); egl-20(mu320)* and *unc-62(mu232); egl-20(mu320)*, but not in double mutants *ceh-20(mu290); mig-13(mu31)* or *unc-62(mu232); mig-13(mu31)*. The penetrance of *mig-13(mu31)* phenotypes is equal to that of the molecular null, *mu225* (Sym et al., 1999). *egl-20(mu320)* is likely a null allele (Ch'ng et al., 2003). Double mutants of *ceh-20(mu290)* or *unc-62(mu232)* with a strong allele of *egl-20*, *n585*, also displayed QR descendants migrating posteriorly instead of anteriorly (histogram not shown). In *ceh-20(mu290); egl-20(n585)* or *unc-62(mu232); egl-20(n585)* double mutants, 24% or 13%, respectively, of QR.pax cells were located in the posterior body between V5.a and V6.a. Distributions of QR.pax cells in *ceh-20(mu290)*, *unc-62(mu232)*, *egl-20(mu320)* and *mig-13(mu31)* single mutants are also shown. There is no significant difference in the QR.pax distributions between *ceh-20(mu290)* and *ceh-20(mu290); mig-13(mu31)* ($P>0.05$). (D) QR.pax cells were displaced further posteriorly in *lin-39(n1760); egl-20(mu320)* and *lin-39(mu26); mig-13(mu31)* double mutants than in *lin-39(n1760)*, *egl-20(mu320)* or *mig-13(mu31)* single mutants. However, QR descendants did not actively migrate towards the posterior in these double mutants. The mutation in *lin-39(mu26)* is predicted to eliminate DNA-binding activity, whereas *lin-39(n1760)* is a null allele lacking the homeodomain (Clark et al., 1993; Wang et al., 1993). *lin-39(mu26)* and *lin-39(n1760)* single mutants have nearly identical QR.pax distributions. The vertical gray line indicates the birthplace of the QR cell. The pink arrow indicates the total anterior distance traversed by QR and its descendants giving rise to QR.pax in wild-type animals. The green arrows denote active posterior migration of cells giving rise to QR.pax. $n=100$ cells for each strain.

distribution seen in *ceh-20* or *unc-62* single mutants, raising the possibility that *ceh-20* and *unc-62* may have a function in the *mig-13* pathway. A *mig-13(mu31null)* mutation can cause cells in the QR lineage to reverse direction and migrate toward the posterior in an *egl-20(-)* background (Fig. 4A) (Harris et al., 1996; Sym et al., 1999). Similarly, in *ceh-20* or *unc-62* double mutants with a null or haploinsufficient allele of *egl-20*, QR.pax cells could be posterior to the birthplace of QR (Fig. 4B,C). However, combining null mutations in *lin-39* and *egl-20* did not

cause cells in the QR lineage to migrate posteriorly (Fig. 4D). In addition, removing *mig-13* activity from *ceh-20(mu290)* or *unc-62(mu232)* did not result in the posterior migration of QR descendants (Fig. 4B,C). Finally, in *ceh-20(mu290); unc-62(mu232)* double mutants, there were QR.pax cells posterior to the birthplace of QR (see Fig. S3 in the supplementary material). Collectively, these results suggest that *ceh-20* and *unc-62*, but not *lin-39*, may act in the same pathway as *mig-13* to promote anterior migration.

To test directly whether *ceh-20* and *unc-62* were required for cells to respond to the anterior-promoting activity of *mig-13*, we asked whether expression of *mig-13::gfp* in our *ceh-20(mu290)* and *unc-62(mu232)* mutants using the pan-neuronal *unc-119* promoter (see Materials and methods) could rescue the shortened anterior migrations of cells in the Q lineage. In *mig-13(null)* and *lin-39(null)* animals, pan-neuronal *mig-13* expression could rescue the QR.pax positioning defect; however, in *ceh-20(mu290)* or *unc-62(mu232)* animals it could not (Fig. 5). In addition, *P_{unc-119}::mig-13* failed to fully rescue a different anterior cell migration, that of BDU, in *ceh-20* and *unc-62* mutants (Fig. 5). In these mutant backgrounds, pan-neuronal expression of *mig-13* could not fully restore anterior

migration of BDU or cells in the QR lineage but could shorten the posterior migration of another cell, CAN (see Fig. S4 in the supplementary material). Thus, we believe that *mig-13* was appropriately misexpressed in these mutants. Together, these results suggest that *ceh-20* and *unc-62*, but not *lin-39*, are required for QR descendants and BDU to respond to the anterior-promoting activity of *mig-13*.

Shortened anterior migration defect of QR descendants in *ceh-20* and *unc-62* mutants is not due to decreased *lin-39* or increased *mab-5* expression in these cells

Another possible explanation for the truncated anterior migration of QR descendants in *ceh-20* and *unc-62* mutants was that cells in the QR lineage inappropriately express the Hox gene *mab-5*. If so, then removing *mab-5* activity in our *ceh-20* or *unc-62* mutants should allow QR descendants to migrate further anteriorly. However, the cell distributions of QR.p descendants in the *mab-5(-)* double mutant with either *ceh-20(mu290)* or *unc-62(mu232)* were nearly indistinguishable from those of *ceh-20(mu290)* or *unc-62(mu232)* single mutants, respectively, indicating that ectopic

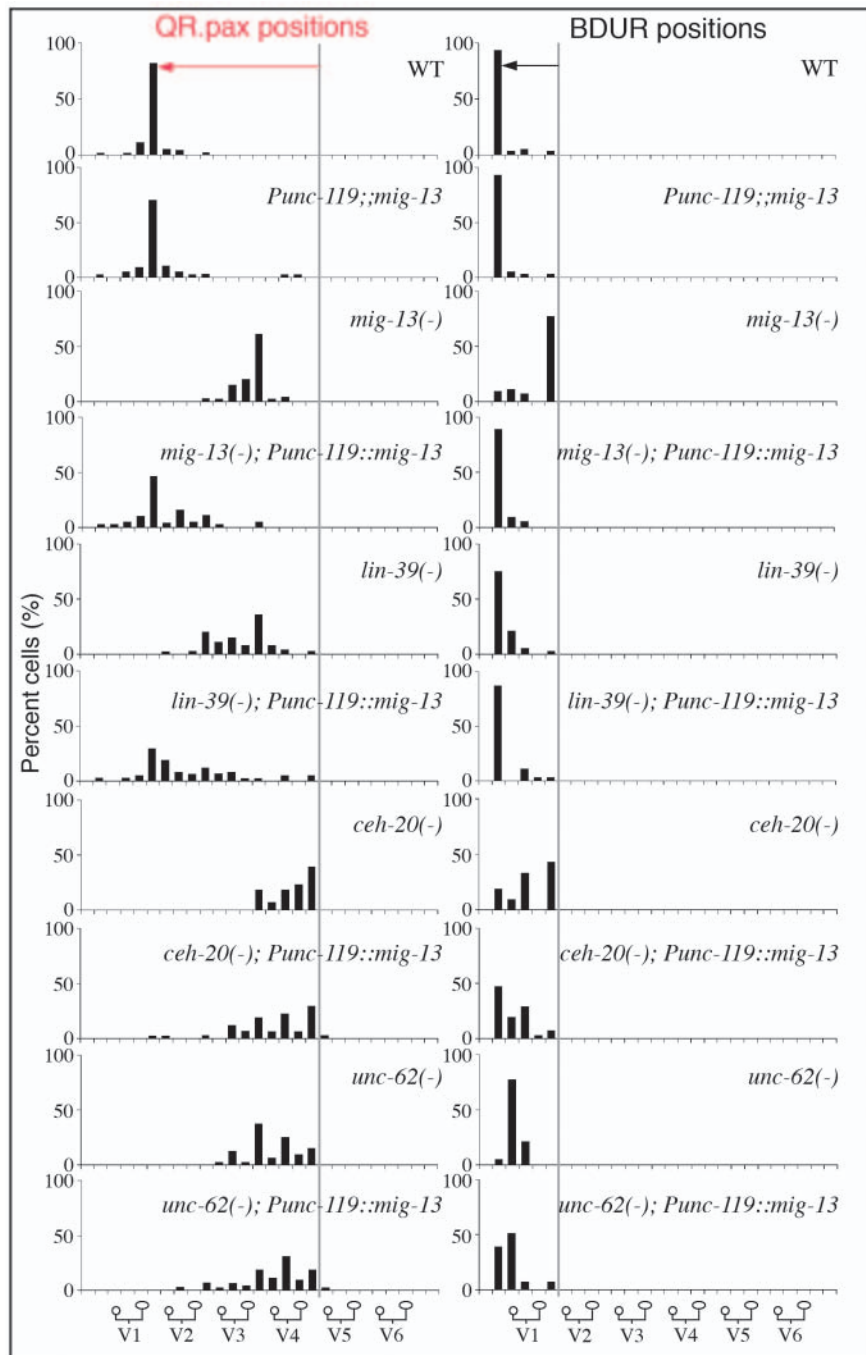


Fig. 5. MIG-13 requires *ceh-20* and *unc-62*, but not *lin-39*, to promote anterior migration. The left column shows the distribution of QR.pax cells in *mig-13(mu225)*, *lin-39(n1760)*, *ceh-20(mu290)* and *unc-62(mu232)* single mutants. Expression of *mig-13* in all neurons under the *unc-119* promoter (*P_{unc-119}::mig-13*) rescues this migration defect in *mig-13(-)* and *lin-39(-)*, but not in *ceh-20(-)* or *unc-62(-)* animals. In an otherwise wild-type background, *P_{unc-119}::mig-13* does not alter the distribution of these cells. The vertical gray line indicates the birthplace of the QR cell. The pink arrow indicates the total anterior distance traversed by QR and its descendants giving rise to QR.pax in wild-type animals. $n=100$ cells for each strain. The right column shows the distribution of the right BDU cell (BDUR) in these same strains at the end of L1. The embryonic migration of BDU starts from the region between V1 and V2 (indicated by the vertical gray line) and ends just anterior to V1 in wild-type animals. The full anterior migration of this cell is blocked in 8% of wild type, 92% of *mig-13(mu225)*, 26% of *lin-39(n1760)*, 82% of *ceh-20(mu290)* and 96% of *unc-62(mu232)* animals. Expression of *mig-13* in all neurons restores full anterior migration in 88% and 86% of *mig-13(mu225)* and *lin-39(n1760)* animals, respectively, but in only 46% and 38% of *ceh-20(mu290)* and *unc-62(mu232)* animals, respectively. In an otherwise wild-type background, *P_{unc-119}::mig-13* does not alter the distribution of BDUR. Similar distributions were observed for the left BDU cell in these strains (data not shown). The black arrow indicates the anterior distance that BDU migrates in wild-type animals. $n=50$ cells for each strain.

Table 1. LIN-39 expression in Q cells and their daughters

Genotype	% animals expressing <i>lin-39</i>								
	QR before delamination <i>n</i> =39 wild type, 40 <i>ceh-20</i> , 32 <i>unc-62</i>			QR after delamination <i>n</i> =40 wild type, 35 <i>ceh-20</i> , 40 <i>unc-62</i>			QR after division <i>n</i> =32 wild type, 33 <i>ceh-20</i> , 38 <i>unc-62</i>		
	Strong	Weak	Absent	Strong	Weak	Absent	Strong	Weak	Absent
Wild type	20.5	20.5	59.0	50.0	45.0	5.0	75.0	25.0	0.0
<i>ceh-20(mu290)</i>	100.0	0.0	0.0	100.0	0.0	0.0	100.0	0.0	0.0
<i>unc-62(mu232)</i>	9.4	34.4	56.2	27.5	67.5	5.0	63.2	34.2	2.6

Genotype	QL before delamination <i>n</i> =40 wild type, 39 <i>ceh-20</i> , 33 <i>unc-62</i>								
	QL after delamination <i>n</i> =37 wild type, 36 <i>ceh-20</i> , 41 <i>unc-62</i>			QL after division <i>n</i> =35 wild type, 41 <i>ceh-20</i> , 38 <i>unc-62</i>					
	Strong	Weak	Absent	Strong	Weak	Absent	Strong	Weak	Absent
Wild type	0.0	32.5	67.5	21.6	27.0	51.4	0.0	17.1	82.9
<i>ceh-20(mu290)</i>	84.6	15.4	0.0	94.4	5.6	0.0	24.4	41.5	34.1
<i>unc-62(mu232)</i>	18.2	81.8	0.0	53.7	46.3	0.0	44.7	55.3	0.0

expression of *mab-5* was unlikely to underlie the migration shortening in these mutants (Fig. 3). In concordance with this finding, *mab-5::lacZ* was not ectopically expressed in QR or its descendants in these mutants (data not shown).

If CEH-20 and UNC-62 do not repress *mab-5* expression in QR descendants, then do they regulate migration of these cells by controlling *lin-39* expression? By staining wild-type animals with an antibody against LIN-39, we show that QR could express *lin-39* in its nucleus before it delaminates from the epithelium, but expression at this early time is usually not high (see Fig. S5A in the supplementary material, Table 1). After delamination but before division, more QR cells expressed *lin-39* strongly (see Fig. S5B in the supplementary material). After QR divides, *lin-39* expression persisted and continued throughout the lineage. In *unc-62(mu232)* animals, *lin-39* expression in QR and its daughters resembled that of wild-type (Table 1). In *ceh-20(mu290)* animals, however, *lin-39* expression was often stronger than that of wild-type in QR before delamination, after delamination and after division (see Fig. S5D-F in the supplementary material, Table 1). Neighboring V and P cells in *ceh-20(mu290)* also had increased LIN-39 staining. These differences were validated in many repeated staining comparing wild-type and *ceh-20(mu290)* animals under identical staining conditions. Because *lin-39* overexpression does not inhibit anterior cell migration in the QR lineage (Hunter and Kenyon, 1995), the altered *lin-39* expression we observed in *ceh-20* mutants was unlikely to contribute to the shortened migrations of these cells.

On the left side, we also observed stronger *lin-39* expression in QL and/or its daughters in *ceh-20(mu290)* and *unc-62(mu232)* mutants (see Fig. S5G-L in the supplementary material; Table 1). In addition, we found that *mab-5* expression was reduced. A *mab-5::lacZ* fusion was expressed in the QL daughters in 72% (*n*=98) of wild-type animals but only in 23% (*n*=39) of *ceh-20(mu290)* animals and 30% (*n*=59) of *unc-62(mu232)* animals. Although this altered expression might have contributed to the anterior migration of the QL.ap cell, it did not affect the position of the QL.pax cells: not only were these cells positioned normally in *ceh-20(mu290)* and *unc-62(mu232)* animals, but addition of either mutation to *mab-5(-)* or *egl-20(-)* shortened the anterior migration of QR.p descendants (see Fig. S6 in the supplementary material).

Mutations in *ceh-20* or *unc-62* disrupt several aspects of vulva formation

In addition to having Q lineage defects, all *ceh-20(mu290)* and *unc-62(mu232)* hermaphrodites were egg-laying defective (Egl). Furthermore, all *ceh-20(mu290)* hermaphrodites formed 'bags of worms' as their progeny hatched internally. Instead of having a single, centrally located vulval protrusion, as in wild-type, 94% (*n*=100) of *ceh-20(mu290)* mutants have multiple vulval protrusions (Muv phenotype) on the ventral surface. We tested whether this phenotype was a loss-of-function phenotype, using RNA interference and found that over 20% (*n*=50) of the progeny of animals fed bacteria expressing *ceh-20* dsRNA had more than one ventral protrusion. This finding, together with our finding that *mu290/+* animals have no ventral protrusions (100%, *n*=132), suggest that *mu290* reduces the level of an activity of *ceh-20* required for normal vulva formation.

Extra ventral protrusions can be caused by ectopic induction of Pn.p cells that do not normally contribute to vulva formation, or by defective morphogenesis (Chen and Han, 2001b; Sternberg and Han, 1998). Examination of vulva development using Nomarski optics revealed that in over 95% of *ceh-20(mu290)* hermaphrodites, Pn.p cells that do not normally undergo vulva development, that is, P3.p, P4.p and/or P8.p, are often ectopically induced to form a vulval invagination (Fig. 6B; Table 2). In addition, anterior and posterior Pn.p cells that normally fuse with the hypodermal syncytium, P(1,2,9-11).p, could also be induced so that their descendants formed a small invagination (Fig. 6C). In the six *ceh-20(mu290)* hermaphrodites lineaged, P1.p divided in two animals, P1.px divided in one animal, P2.p divided in four animals, P2.px divided in one animal, P3.px divided in three animals and P8.px divided in one animal. In one animal, not only were the great-granddaughters of P4.p inappropriately generated, but one even divided despite the fact that even the great-granddaughters of P(5-7).p do not normally divide. In contrast to these ectopic inductions, vulval precursor cells that are normally induced, P(5-7).p, were sometimes not induced in *ceh-20(mu290)* hermaphrodites (Table 2). When they were induced, P(5 or 7).p descendants could form invaginations separate from the one formed by the P6.p descendants (Fig. 6B), suggesting that P5.p or P7.p descendants sometimes failed to migrate toward P6.p descendants during morphogenesis

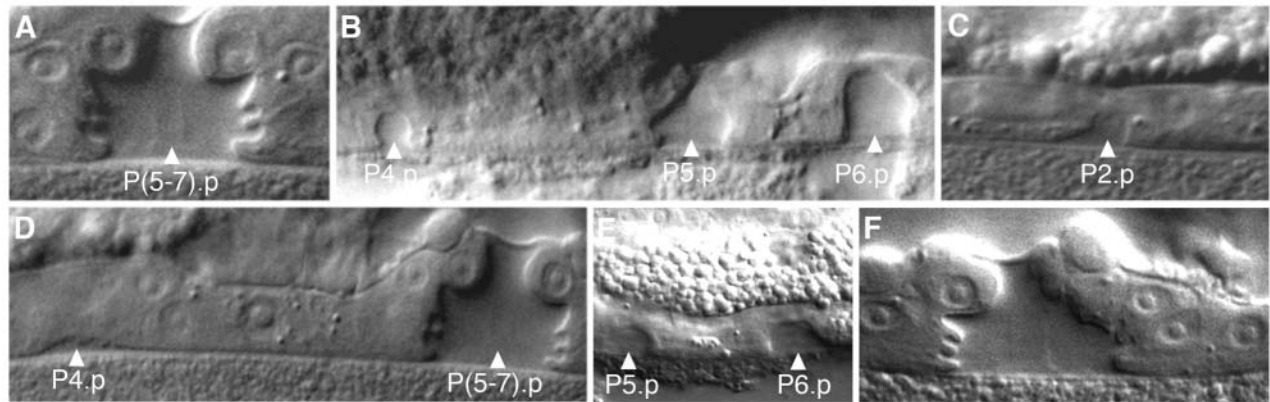


Fig. 6. The Muv phenotype in *ceh-20(mu290)* animals. Nomarski photomicrographs of L4 larvae. (A) Wild-type animal showing a normal vulval invagination formed by P(5-7).p (arrowhead). (B) *ceh-20(mu290)* animal showing separate invaginations formed by P5.p and P6.p while P7.px (not shown) failed to divide further. P4.p also formed a small invagination. (C) *ceh-20(mu290)* animal showing an invagination at P2.p in addition to the invagination formed by P(5-7).p (not shown). (D) *ceh-20(RNAi)* animal showing P4.p forming a separate invagination adjacent to the invagination formed by P(5-7).p. (E) *ceh-20(mu290) lin-39(n1760)* animal showing separate invaginations formed by P5.p and P6.p. P7.p did not divide in this animal. (F) *unc-62(mu232)* animal showing the incomplete migration of some P7.p descendants towards P6.p descendants, resulting in the asymmetric invagination. Animals in all panels are oriented with anterior towards the left.

Table 2. Effects of decreasing *ceh-20* activity on vulval induction

Genotype	n	Induction (%)										Number induced VPCs	
		P1.p	P2.p	VPCs						P9.p	P10.p		P11.p
				P3.p	P4.p	P5.p	P6.p	P7.p	P8.p				
Wild type	25	0	0	0	0	100	100	100	0	0	0	0	3.0±0.0
<i>ceh-20(RNAi)</i>	25	0	0	4	8	100	100	100	0	0	0	0	2.8±0.6
<i>ceh-20(mu290)</i>	23	9	22	65	61	78	91	43	56	4	4	4	2.0±0.5
<i>lin-39(n1760)</i>	25	0	0	0	0	0	0	0	0	0	0	0	0.0±0.0
<i>ceh-20(mu290) lin-39(n1760)</i>	26	0	4	8	4	15	58	8	0	0	0	0	0.5±0.4

(48%, $n=50$). Curiously, P7.p descendants formed a separate invagination or failed to fully migrate towards P6.p descendants in ~40% of *unc-62(mu232)* (Fig. 6F) and ~50% of *unc-62(ku234)* hermaphrodites ($n=25$ per strain). This defect probably contributes not only to their Egl phenotype but also to the 8% of animals of each strain which had an extra ventral protrusion ($n=100$ per strain). In *ceh-20(RNAi)* animals, we also observed ectopic induction of P3.p and P4.p (Fig. 6D, Table 2) as well as separate invaginations formed by P5.p or P7.p (10%, $n=50$). Thus, both ectopic induction and defective morphogenesis contribute to the multiple ventral protrusions in hermaphrodites with reduced CEH-20 activity, and UNC-62 activity is also required for proper morphogenesis.

ceh-20(mu290) mutants also displayed vulval lineage defects. In wild-type animals, P6.p adopts the primary fate, the fate in which all granddaughters divide transversely to generate eight descendants (reviewed by Greenwald, 1997). P5.p and P7.p normally adopt the secondary fate to generate seven descendants each. Their granddaughters divide longitudinally (L), transversely (T) or not at all (N), depending on their positions along the anteroposterior axis (from anterior to posterior, LLTN for P5.p and NTLL for P7.p). In *ceh-20(mu290)* animals, the induced Pn.p cells rarely generated the eight or seven descendants characteristic of primary or secondary fates, respectively. Out of 23 animals, there was only one animal in which P6.p had divided to generate eight cells. All of the other animals had fewer than eight P6.p descendants,

and all of the animals had fewer than the expected seven descendants of P5.p and P7.p in the L4 stage. We confirmed that vulval cell divisions are prematurely truncated in *ceh-20(mu290)* animals by lineage analysis. In two of the six *ceh-20(mu290)* hermaphrodites lineaged, at least one of the P(5-7).p daughters failed to divide. Furthermore, at least one of the P(5-7).p granddaughters that normally divide failed to divide in two animals. In addition to the premature truncation of vulval lineages, cells could also divide along an unusual axis in *ceh-20(mu290)* animals. In one of the six *ceh-20(mu290)* hermaphrodites lineaged, all six P6.p granddaughters divided longitudinally instead of transversely. In this same animal, P5.pppa divided obliquely instead of transversely, P7.pppa divided obliquely instead of longitudinally, and both P5.ppp and P7.pppa divided obliquely instead of remaining undivided. Taken together, these observations suggest that *ceh-20* is also required for proper execution of VPC fates.

Because the extreme anterior and posterior Pn.p cells, (P1,2,9-11).p, often divided in *ceh-20(mu290)* mutants, we hypothesized that these cells failed to fuse to the hypodermal syncytium in mutant animals. To characterize this defect better, we used the *jam-1::GFP* marker, which labels cell adhesion junctions of unfused, but not fused, Pn.p cells (Mohler et al., 1998). In wild-type hermaphrodites, only P(3-8).p remain unfused after the early fusion event during L1. P3.p fuses by L3 in ~50% of wild-type animals. In *ceh-20(mu290)* hermaphrodites, as in wild-type, the six central Pn.p cells

Table 3. Effects of decreasing *ceh-20* and *unc-62* activity on Pn.p cell fusion**(A) Unfused Pn.p cells after the early fusion event (%)**

Genotype	Number of cells										
	1	2	3	4	5	6	7	8	9	10	11
Wild type	0	0	100	100	100	100	100	100	0	0	2
<i>ceh-20(mu290)</i>	8	36	100	100	100	100	100	100	100	98	88
<i>unc-62(mu232)</i>	0	4	100	100	100	100	100	90	4	4	20

(B) Unfused Pn.p cells after the late fusion event (%)

Genotype	Number of cells										
	1	2	3	4	5	6	7	8	9	10	11
Wild type	0	0	48	100	100	100	100	100	0	0	0
<i>ceh-20(mu290)</i>	12	44	100	100	100	100	100	100	92	84	88
<i>unc-62(mu232)</i>	5	10	90	100	100	100	100	100	10	10	25

n=50 per strain at each time point.

remained unfused, but P1.p, P2.p and P(9-11).p sometimes also failed to fuse during the early fusion event (Table 3A). Some anterior and posterior Pn.p cells, as well as P3.p, still remained unfused in the L3 stage (Table 3B), suggesting that CEH-20 activity is required to generate the proper number of VPCs. Like *ceh-20(mu290)* animals, *unc-62(mu232)* hermaphrodites also exhibited the Pn.p cell fusion defect, although with lower penetrance (Table 3).

The Hox gene *lin-39* is required during the L1/L2 stage for the P(3-8).p cells to remain unfused, and, later, to generate vulval cell divisions (Clandinin et al., 1997; Clark et al., 1993; Shemer and Podbilewicz, 2002; Wang et al., 1993). In *lin-39(null)* animals, P(3-8).p cells all fuse, causing the animals to be vulvaless. To ask whether the *ceh-20* Muv phenotype might result from altered *lin-39* activity, we examined vulva development in *ceh-20(mu290) lin-39(n1760null)* double mutants. Surprisingly, though the number of protrusions was reduced, we found that 44% (*n*=100) of these animals had one or more ectopic ventral protrusions. It is probable that these protrusions arose, in part, from ectopic induction of P.3p and P4.p, as well as P2.p in these double mutants (Table 2). When P5.p or P7.p were induced, their descendants sometimes failed to migrate towards the descendants of P6.p, resulting in a separate invagination (Fig. 6E). Thus, the Muv phenotype of *ceh-20* mutants is at least partially independent of LIN-39.

***ceh-20* and *unc-62* also pattern V cells**

A row of six lateral hypodermal cells (V1-V6) runs along each side of newly hatched wild-type animals. During the first larval stage, each V cell divides asymmetrically along the AP axis, generating an anterior daughter (Vn.a) that fuses with hyp7 and a posterior daughter (Vn.p) that adopts the seam cell fate and continues to divide (Sulston and Horvitz, 1977).

We found that the nuclei of the anterior daughters of some V cells were sometimes replaced by two small nuclei in *ceh-20(mu290)* animals, and more often in *unc-62(mu232)* animals (see Fig. S7 in the supplementary material, Table 4). We determined that the two small nuclei were indeed daughters of Vn.a cells by lineage analysis (data not shown). These cells did not express a seam-specific GFP marker (Koh and Rothman, 2001) and thus were not transformed into Vn.p-like seam cells (data not shown). Instead, these cells appeared to fuse with hyp7: first, the adherens-junction marker *jam-1::GFP* failed to

label these cells at the L2 stage (data not shown); and second, we determined the lineage of a dividing Vn.a cell in an *unc-62(mu232)* animal harboring *jam-1::GFP* and found that there was only a short period of time when Vn.ax cells were outlined in green (see Fig. S8 in the supplementary material). Because the cell outlines of Vn.ax can be observed, albeit transiently, Vn.a division occurs before fusion. Whether *ceh-20* and *unc-62* actively inhibit cell division or simply promote fusion of Vn.a cells so that cell division cannot occur is currently unknown.

In addition to these defects, we found that in *unc-62(mu232)* animals, V5.a was often completely missing and replaced by neuronal cells (see Fig. S9 in the supplementary material). Lineage analysis of V5.a on the right (*n*=2) and left (*n*=1) sides in *unc-62(mu232)* animals showed that V5.a could generate a Q-like lineage pattern, producing three migratory cells. Using *mec-7::gfp* which is expressed in six differentiated cells including Q.paa, we confirmed that in *unc-62(mu232)* animals, V5.a descendants can express a fate marker normally expressed in Q descendants (data not shown).

***ceh-20* is expressed in Q, P, and V cells and their descendants**

We constructed a *ceh-20::gfp* translational fusion gene (pLY11) to investigate where and when *ceh-20* is expressed. Transgenic *ceh-20(mu290)* animals bearing pLY11 were rescued for the QR.pax positioning phenotype, the Muv/Egl,

Table 4. Effects of decreasing *ceh-20* and *unc-62* activity on Vn.a cell division

Genotype	Side	Number of divided Vn.a cells (%)					
		V1.a	V2.a	V3.a	V4.a	V5.a	V6.a
Wild type	L	0	0	0	0	0	0
	R	0	0	0	0	0	0
<i>ceh-20(mu290)</i>	L	10	0	0	0	0	0
	R	16	0	0	0	0	0
<i>unc-62(mu232)</i>	L	54	24	0	4	30	12
	R	86	44	0	6	28	22
<i>ceh-20(mu290); unc-62(mu232)</i>	L	88	88	52	56	74	64
	R	82	74	42	52	60	82

n=50 per strain per side.
L, left; R, right.

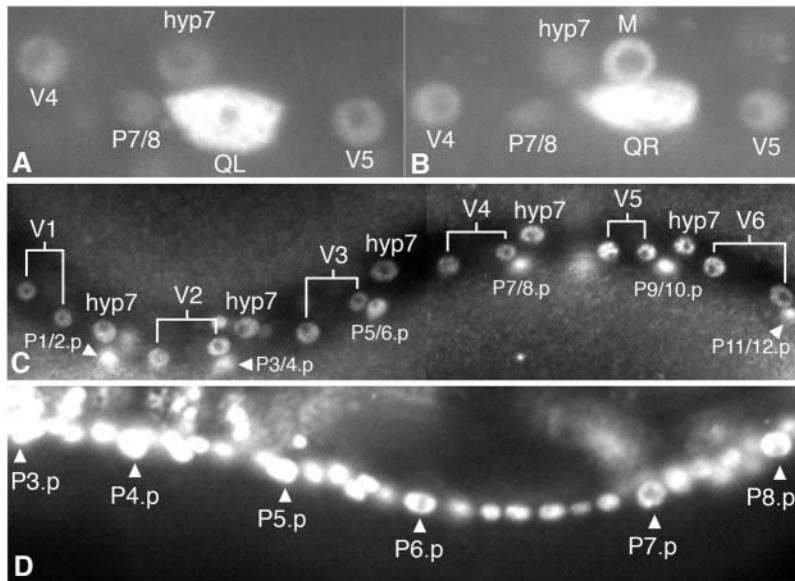


Fig. 7. *ceH-20* is expressed in nuclei of Q, P and V cells and their descendants. (A-C) Fluorescence micrographs of wild-type larvae carrying *ceH-20::gfp*. This plasmid rescued the cell migration defects (QL and QR descendants, BDU) and the multivulval defect of *ceH-20(mu290)* animals. Dorsal is upwards and anterior is towards the left. (A,B) At hatching, *ceH-20* is expressed in the nuclei of ectodermal such as the Q cells, P cells, V cells and hyp7. The mesodermal precursor, M, also expresses *ceH-20* robustly. (C) Six to eight hours after hatching, V cell daughters, hyp7 cells and P cells continue to express *ceH-20*. In this animal, the right side is shown. The descendants of QR have migrated anteriorly and are in the process of dividing (not visible by fluorescence). (D) In this L2 animal, P(1-11).p cells express *ceH-20*, although only P(3-8).p are shown. Ventral cord neurons between the Pn.p cells also express *ceH-20::gfp*.

and the Vn.a division phenotype, suggesting that *ceH-20::gfp* was expressed in cells that require its function for these processes. In all cells expressing *ceH-20*, the expression was stronger in the nucleus than in the cytoplasm. We detected *ceH-20::gfp* expression in QR and QL (Fig. 7A,B) and their descendants throughout their migrations to the end of L1. V cells and their daughters also expressed *ceH-20::gfp* (Fig. 7A-C). Expression persisted in the descendants of the V cells through the adult stage (data not shown). At hatching, all P cells expressed *ceH-20::gfp* (Fig. 7A,B). Before the anterior and posterior Pn.p cells fuse, they also expressed *ceH-20*. In L3 hermaphrodites, expression was maintained in P(3-8).p (Fig. 7D). We identified *ceH-20::gfp* expression in several other cell types. These included M, BDU, ALM, HSN, body wall muscle cells, I4, all L1 ventral cord neurons and a few unidentified neurons in the head behind the posterior bulb of the pharynx. *ceH-20::gfp* expression and nuclear localization did not change in the *unc-62(mu232)* background (data not shown).

Discussion

The *C. elegans* orthologs of Hox co-factors Exd/Pbx (*ceH-20*) and Hth/Meis/Prep (*unc-62*), have been shown previously to play an important role in the post-embryonic development of the mesoderm and the embryo, respectively (Liu and Fire, 2000; Van Auken et al., 2002). In this study, we provide evidence that *ceH-20* and *unc-62* are also required for the post-embryonic development of the ectoderm, including the Q, V

and P cell lineages. Our analyses of *ceH-20* and *unc-62* mutants indicate that they play a crucial role in ensuring that these cells and their descendants undergo their invariant patterns of cell division, migration, fusion and morphogenesis. Some, but not all, of the *ceH-20* and *unc-62* mutant ectodermal phenotypes resemble those of Hox gene *lin-39* mutants. Thus, CEH-20 and UNC-62 could conceivably function as *lin-39* co-factors in some of the cell-fate decisions they influence, but probably not in others.

CEH-20 and UNC-62 are required for a step in Q cell migration that involves the transmembrane protein MIG-13

Our interest in these *ceH-20* and *unc-62* mutants was initially stimulated by the fact that their cell migration phenotypes are quite similar to those produced by loss-of-function mutations of the transmembrane protein MIG-13 (Sym et al., 1999). Mutations in all of these genes prevented the anteriorwards migration of BDU and severely shortened the anteriorwards migration of the QR descendants. Moreover, we found that our *ceH-20* and *unc-62* mutations, in combination with other Q migration mutants, produced phenotypes similar to those we had seen previously with *mig-13*. For example, combining a *unc-62* or *ceH-20* mutation with a *lin-39* null allele abolished nearly all anteriorwards migration of the Q descendants. Combining an *unc-62* or *ceH-20* mutation with an *egl-20/Wnt* null mutation could cause cells in the QR lineage to reverse direction and migrate posteriorly rather than anteriorly. Finally, we found that global overexpression of MIG-13 was unable to stimulate anteriorwards migration in *ceH-20* or *unc-62* mutant backgrounds. Together, these findings suggest that, in Q cell migration, *ceH-20* and *unc-62* may function in the same regulatory step as MIG-13. The possibility that *ceH-20* and *unc-62* are simply required for *mig-13* expression is ruled out by the finding that these *ceH-20* and *unc-62* mutations do not affect the pattern of MIG-13::GFP (data not shown). Because CEH-20 and UNC-62 are known to regulate transcription, one possibility is that they regulate the expression of another, as yet unidentified, molecule that functions in the same process as MIG-13 to promote anteriorwards migration. Alternatively, CEH-20 and UNC-62 may act in a pathway that is independent of and parallel to other pathways involving LIN-39, MIG-13, and EGL-20. Our data would also be consistent with such a model in which CEH-20 and UNC-62 act in a pathway that is dominant over these other pathways, increasing the difficulty with which *mig-13* overexpression rescues the shortened anterior migration in *ceH-20* or *unc-62* mutant animals. Determining which cells require *ceH-20* and *unc-62* for proper Q descendant migration and identifying *ceH-20* and *unc-62* effector(s) may facilitate the understanding of mechanisms that regulate cell migration along the anteroposterior axis in *C. elegans*.

Roles of *ceH-20* and *unc-62* in vulva development

Our genetic studies of *ceH-20* and *unc-62* demonstrate that they

play multiple roles in regulating vulva development. First, in *ceh-20* and *unc-62* single mutants, cells anterior and posterior to the VPCs sometimes fail to fuse with the syncytial hypodermis. Although ectopic *lin-39* expression could explain this phenotype, it does not, because, as in wild type, *lin-39* is expressed in only the six central Pn.p cells in *ceh-20* and *unc-62* mutants even when some anterior and posterior Pn.p cells are unfused (data not shown). Thus, UNC-62 and CEH-20 appear to regulate cell fusion independently of LIN-39. Second, *ceh-20* is required to prevent cells outside of the vulval equivalence group from generating vulval cell lineages and also for ensuring that the central VPCs do generate vulval cell lineages. Consistent with this, ~26% of P6.p cells in L3 *ceh-20(mu290)* hermaphrodites (versus 0% in wild-type) fail to express *egl-17::gfp*, an early marker for the primary fate (data not shown). Although we did not see induction and/or lineage defects in *unc-62(mu232)* mutants, it is probable that *unc-62* is also involved in these processes since non-vulval VPC descendants and vulval-like descendants of Pn.p cells outside of the vulval equivalence group have been observed when a weak *unc-62* allele has been placed over a *unc-62(null)* or a deficiency encompassing the *unc-62* gene (Van Auken et al., 2002). In addition, cell divisions of P(5-7).p were often prematurely terminated or misoriented in *ceh-20(mu290)* hermaphrodites, suggesting that CEH-20 is required for the proper execution of the primary and secondary vulval fates. Finally, in *ceh-20* and *unc-62* mutants, the descendants of P5.p and P7.p sometimes failed to migrate towards the descendants of P6.p (Fig. 6) (Van Auken et al., 2002), indicating that proper morphogenesis of the VPC descendants requires CEH-20 and UNC-62 activity. Thus, both *ceh-20* and *unc-62* participate in multiple steps in vulva formation.

The vulval phenotypes exhibited by *ceh-20(mu290)* animals are reminiscent of those in NuRD complex mutants such as *lin-40* MTA (metastasis associated factor) and *hda-1* HDAC (histone deacetylase). Like *ceh-20(mu290)* animals, *lin-40* or *hda-1* mutants also have disrupted axes of transverse divisions, and their P5.p and P7.p descendants may form a separate invagination (Chen and Han, 2001b; Dufourcq et al., 2002). Animals doubly mutant for *lin-40* and a class B synMuv gene also exhibit underinduction of P(5-7).p and overinduction of P(3,4,8).p (Chen and Han, 2001b). In addition, mutating *lin-40* increases the frequency of unfused P3.p cells, and, in an *egl-27* MTA mutant background, a *lin-40* mutation causes posterior P(9-11).p cells to also remain unfused (Chen and Han, 2001a).

We note that whereas the VPCs remained unfused in our *ceh-20(mu290)* animals, these cells have been reported to fuse with *hyp7* in *ceh-20(ay42)* mutants (Shemer and Podbilewicz, 2002). One possible explanation for this discrepancy is that, although both mutations alter residues in the conserved homeodomain, they may disrupt different functions of *ceh-20*: *mu290* changes a residue that is predicted to form hydrogen bonds with the guanine of the TGAT core in the major groove of the DNA, whereas *ay42* changes a residue that is predicted to contact the Hox protein (E. Chen, PhD thesis, Yale University, 1996) (Passner et al., 1999; Piper et al., 1999).

How might *ceh-20* and *unc-62* interface with known regulators of vulva development? It has been shown that CEH-20, together with LIN-39, participates in Pn.p fusion by regulating the expression of fusion effector *eff-1* and GATA factors *egl-18* and *elt-6* (Koh et al., 2002; Shemer and

Podbilewicz, 2002). Our findings suggest that CEH-20 and UNC-62 may have additional functions during vulva formation. The *C. elegans* NuRD complex components repress transcription during vulval fate specification by regulating chromatin structure (Ahringer, 2000). A recent study demonstrated that in mammalian cells, the *ceh-20* homolog PBX1 can interact with histone deacetylase HDAC (Saleh et al., 2000b). By analogy to their mammalian counterparts, CEH-20 might interact with HDA-1 (HDAC). Thus, in general terms, our findings raise the possibility that CEH-20 and UNC-62 are required either for the expression of specific NuRD complex proteins, or for the proper function of the NuRD complex during vulva development (see L. Yang, PhD thesis, University of California, San Francisco, 2003). Future work analyzing the relationships between *ceh-20*, *unc-62*, and NuRD complex components may provide a more comprehensive view on how vulva development is controlled in *C. elegans*.

CEH-20 and UNC-62 may act independently of Hox protein LIN-39 in some processes regulated by all three genes

Mutations in *ceh-20* and *unc-62* affect processes that Hox gene *lin-39* also affects, such as cell migration and vulva development. Because *ceh-20* and *unc-62* have been shown to act as Hox co-factors in the *C. elegans* mesoderm and embryo (Liu and Fire, 2000; Van Auken et al., 2002), we considered the possibility that the *ceh-20(mu290)* and *unc-62(mu232)* phenotypes could be caused by altered target-site specificity of LIN-39. However, based on the many phenotypic differences we observe between *ceh-20(mu290)* or *unc-62(mu232)* and *lin-39(n1760)* animals, it is probable that *ceh-20* and *unc-62* have functions that are at least partly independent of *lin-39* in the ectoderm.

Some of the Ceh-20 and Unc-62 phenotypes we observed were initially suggestive of a LIN-39-co-factor role for CEH-20 and UNC-62. For example, in *ceh-20(mu290)*, *unc-62(mu232)* and *lin-39(null)* mutants, anterior migrations of QR descendants are shortened. Consistent with this, *ceh-20* is expressed in the nucleus of QR and its descendants where *lin-39* acts autonomously (Clark et al., 1993; Wang et al., 1993). In vulva development, our observation that P(5-7).p cell divisions sometimes terminated prematurely in *ceh-20(mu290)* animals is reminiscent of that seen in *lin-39* mutants under conditions in which VPC fusion to the hypodermis was prevented and in animals with reduced activity of a LIN-39 target, *egl-18* (Koh et al., 2002; Shemer and Podbilewicz, 2002).

Other phenotypes, however, suggest that *ceh-20* and *unc-62* may function somewhat independently in processes that *lin-39* also regulates. For example, QR descendants migrate further anteriorly in *lin-39(null)* mutants than in *ceh-20(mu290)* or *unc-62(mu232)* animals. In addition, unlike *ceh-20(mu290)* or *unc-62(mu232)* animals, *lin-39(null)* mutants do not share the shortened BDU migration phenotype with *mig-13* mutants or exhibit QR descendants migrating in the wrong direction in the absence of *egl-20* (Harris et al., 1996; Sym et al., 1999). Furthermore, ectopic *mig-13* expression can rescue the anterior migration defect of QR descendants in *lin-39(null)* animals but not in *ceh-20(mu290)* or *unc-62(mu232)* animals. For this reason, the hypothesis that *ceh-20* and *unc-62* act in a *mig-13*-dependent process rather than a strictly *lin-39*-dependent

process seems reasonable. Although it is theoretically possible that another *C. elegans* homolog of *exd*, *ceh-40*, is also involved in this process, we have observed no migration phenotypes upon RNA interference of *ceh-40* in the *rrf-3* background, and no enhancement of migration phenotypes in the *ceh-20*; *rrf-3* background (data not shown).

In vulva development, we observed that many *ceh-20(mu290)* and *ceh-20(RNAi)* hermaphrodites, and some *unc-62(mu232)* animals, are multivulval, whereas *lin-39(null)* mutants are vulvaless. Removing *lin-39* activity causes all Pn.p cells, including P(3-8).p, to fuse in late L1 (Clark et al., 1993; Wang et al., 1993). By contrast, in *ceh-20(mu290)* and *unc-62(mu232)* mutants, P(3-8).p remain unfused as in wild type, and Pn.p cells that normally fuse sometimes fail to fuse. In *lin-39(null)* animals rescued for the early fusion defect, P(5-7).p often fail to complete their lineages, but induction of P(3,4,8).p has not been observed (Maloof and Kenyon, 1998). In *ceh-20(mu290)* and *ceh-20(RNAi)* animals, however, P(3,4,8).p could also be induced, and, for *ceh-20(mu290)*, this ectopic induction could occur even in a *lin-39(null)* background (Table 2). In addition, *ceh-20* and *unc-62* have a role in vulval morphogenesis (Fig. 6), whereas *lin-39* has been shown to have no role in promoting cell migration during vulva formation (Shemer and Podbilewicz, 2002).

Although it has previously been shown that CEH-20/LIN-39 heterodimers bind enhancers of GATA factors that regulate P(3-8).p fusion (Koh et al., 2002) and that CEH-20 and LIN-39 together repress the fusion effector *eff-1* (Shemer and Podbilewicz, 2002), we hypothesize that *ceh-20* and *unc-62* have some functions that are independent of *lin-39* for vulva formation based on the stark differences in their phenotypes. We speculate that there are partners for CEH-20 and UNC-62 besides LIN-39 in the Pn.p lineages. As vulval phenotypes have not been shown for other *C. elegans* Hox gene loss-of-function mutants, it is possible that CEH-20 pairs with a non-Hox homeodomain protein. There is precedence for this, because a *Drosophila* ortholog of CEH-20, EXD acts as a co-factor for the non-Hox homeodomain protein Engrailed (Peifer and Wieschaus, 1990; van Dijk and Murre, 1994).

Comparison of *ceh-20* and *unc-62* with their *Drosophila* and vertebrate homologs

Do *ceh-20* and *unc-62* function in similar ways as their homologs? First, previous studies in *Drosophila* and vertebrates have demonstrated that the phenotypes produced by mutations in the homologs of *ceh-20* and *unc-62* resemble one another. For example, in *Drosophila*, *exd* and *hth* mutants both exhibit posterior transformations of embryonic segments (Peifer and Wieschaus, 1990; Rieckhof et al., 1997). In zebrafish, mutations in either *lazarus* or *meis* (the *exd* and *hth* homologs, respectively) cause defects in hindbrain segmentation (Choe et al., 2002; Popperl et al., 2000; Waskiewicz et al., 2001; Waskiewicz et al., 2002). Here, we show that this property of these genes is conserved: mutations in *C. elegans ceh-20* and *unc-62* both disrupt, in similar ways, the migration of Q descendants, Pn.p fusion, vulval morphogenesis and the patterning of V cell descendants.

Second, as mentioned above, in many situations, mutations in Hox co-factor genes produce phenotypes that mimic those of Hox mutants. In fact, *Drosophila exd* and *hth* were identified based on their sharing embryonic segmentation defects with

Hox mutants (Peifer and Wieschaus, 1990; Rieckhof et al., 1997). In *C. elegans*, although there are some similarities between the Q migration defects of *unc-62*, *ceh-20* and Hox gene mutants, the details of their phenotypes are very different. The same holds true for vulva development. Thus, *ceh-20* and *unc-62* may have functions independent of *lin-39* in anteriorwards migration and vulva development. In *Drosophila*, Hox-independent functions of *exd* and *hth* have been demonstrated for antennal formation (Casares and Mann, 1998; Yao et al., 1999). However, in contrast to the *C. elegans* situation in which *lin-39* is required and expressed in the cells with defects in migration, fusion or division, *Drosophila* Hox genes are neither required nor expressed in the eye-antennal disc from which the antenna forms (Casares and Mann, 1998; Clark et al., 1993; Wang et al., 1993; Yao et al., 1999).

Third, Hox gene expression is regulated, in part, by Hox co-factors. In *Drosophila*, *exd* and *hth* are required to maintain *Sex-combs reduced* expression in the salivary gland (Henderson and Andrew, 2000). In zebrafish, Hox genes interact with their co-factors to cross-regulate the expression of other Hox genes (Maconochie et al., 1997; Popperl et al., 1995; Studer et al., 1998). As a result, reducing the function or altering the intracellular localization of zebrafish *lazarus* or *meis/prep* genes resulted in decreased expression of various Hox genes. (Choe et al., 2002; Popperl et al., 2000; Waskiewicz et al., 2001). In *C. elegans*, although *ceh-20* does not activate *mab-5* or *lin-39* expression in the mesoderm, it is required for the autoregulatory expression of *ceh-13*, the *C. elegans* ortholog of *Drosophila* Hox gene *labial* (Liu and Fire, 2000; Streit et al., 2002). We found that *lin-39* expression was upregulated, instead of downregulated, in the Q cells of some animals with reduced *ceh-20* or *unc-62* function. Although this was somewhat unexpected, it is possible that *ceh-20* and *unc-62* downregulate Hox gene expression in conjunction with non-HOX proteins downstream of signaling pathways. Although the wingless and the TGF β pathways have not been shown to inhibit Hox gene expression, they do influence Hox gene expression in *C. elegans* (Stoyanov et al., 2003; Streit et al., 2002). Because *lin-39* upregulation was not restricted to the Q cells in *ceh-20* or *unc-62* mutants, we raise the possibility that *ceh-20* and *unc-62* could function with repressors of *lin-39* expression such as SAM domain proteins (Zhang et al., 2003).

Taken together, these comparisons suggest that *C. elegans ceh-20* and *unc-62* share many properties with their homologs, but the degree to which the Hox-independent and Hox-dependent roles of these genes and their homologs dominate may differ in different organisms and even between different tissues within the same organism.

We thank Joy Alcedo, Scott Alper, Javier Apfeld, Queelim Ch'ng, Douglas Crawford, Natasha Libina, Yung Lie, Jennifer Whangbo, Lisa Williams and other members of the Kenyon laboratory for technical advice, supportive environment, stimulating discussions and critical comments on the work. We especially thank Natasha Libina for her expertise in preparing figures for publication. We thank Yung Lie for *rrf-3(pk1426)*; *mul35*, Queelim Ch'ng for *P_{unc-119}::mig-13* and Andy Dillin for the control RNAi vector. We also thank the Sanger Center for cosmids and the CGC for numerous strains. In addition, we are indebted to Michael Stern for providing the *egl-17* promoter, unpublished data and *ceh-20* alleles. We are also grateful to William Wood and Barbara Robertson for communicating unpublished results and for additional *unc-62* alleles. We thank Meera Sundaram for *unc-*

62(*ku234*). Finally, we thank Cori Bargmann for her excellent advice and her laboratory for reagents. L.Y. was supported by the Medical Scientist Training Program (NIH-NIGMS GM07618). M.S. was supported by a postdoctoral fellowship from the Jane Coffin Childs Fund for Medical Research. This work was supported by NIH grant GM37053 to C.K.

Supplementary material

Supplementary material for this article is available at <http://dev.biologists.org/cgi/content/full/132/6/1413/DC1>

References

- Abu-Shaar, M., Ryoo, H. D. and Mann, R. S. (1999). Control of the nuclear localization of Extradenticle by competing nuclear import and export signals. *Genes Dev.* **13**, 935-945.
- Ahringer, J. (2000). NuRD and SIN3 histone deacetylase complexes in development. *Trends Genet.* **16**, 351-356.
- Brehm, A., Miska, E. A., McCance, D. J., Reid, J. L., Bannister, A. J. and Kouzarides, T. (1998). Retinoblastoma protein recruits histone deacetylase to repress transcription. *Nature* **391**, 597-601.
- Brenner, S. (1974). The genetics of *Caenorhabditis elegans*. *Genetics* **77**, 71-94.
- Burglin, T. R. and Ruvkun, G. (1992). New motif in PBX genes. *Nat. Genet.* **1**, 319-320.
- Casares, F. and Mann, R. S. (1998). Control of antennal versus leg development in *Drosophila*. *Nature* **392**, 723-726.
- Chalfie, M. and Sulston, J. (1981). Developmental genetics of the mechanosensory neurons of *Caenorhabditis elegans*. *Dev. Biol.* **82**, 358-370.
- Chen, Z. and Han, M. (2001a). *C. elegans* Rb, NuRD, and Ras regulate lin-39-mediated cell fusion during vulval fate specification. *Curr. Biol.* **11**, 1874-1879.
- Chen, Z. and Han, M. (2001b). Role of *C. elegans* lin-40 MTA in vulval fate specification and morphogenesis. *Development* **128**, 4911-4921.
- Ch'ng, Q., Williams, L., Lie, Y. S., Sym, M., Whangbo, J. and Kenyon, C. (2003). Identification of genes that regulate a left-right asymmetric neuronal migration in *Caenorhabditis elegans*. *Genetics* **164**, 1355-1367.
- Choe, S. K., Vlachakis, N. and Sagerstrom, C. G. (2002). Meis family proteins are required for hindbrain development in the zebrafish. *Development* **129**, 585-595.
- Clandinin, T. R., Katz, W. S. and Sternberg, P. W. (1997). *Caenorhabditis elegans* HOM-C genes regulate the response of vulval precursor cells to inductive signal. *Dev. Biol.* **182**, 150-161.
- Clark, S. G., Chisholm, A. D. and Horvitz, H. R. (1993). Control of cell fates in the central body region of *C. elegans* by the homeobox gene lin-39. *Cell* **74**, 43-55.
- Dufourcq, P., Victor, M., Gay, F., Calvo, D., Hodgkin, J. and Shi, Y. (2002). Functional requirement for histone deacetylase 1 in *Caenorhabditis elegans* gonadogenesis. *Mol. Cell Biol.* **22**, 3024-3034.
- Eisenmann, D. M., Maloof, J. N., Simske, J. S., Kenyon, C. and Kim, S. K. (1998). The beta-catenin homolog BAR-1 and LET-60 Ras coordinately regulate the Hox gene lin-39 during *Caenorhabditis elegans* vulval development. *Development* **125**, 3667-3680.
- Fay, D. S. and Han, M. (2000). The synthetic multivulval genes of *C. elegans*: functional redundancy, Ras-antagonism, and cell fate determination. *Genesis* **26**, 279-284.
- Ferguson, E. L. and Horvitz, H. R. (1989). The multivulva phenotype of certain *Caenorhabditis elegans* mutants results from defects in two functionally redundant pathways. *Genetics* **123**, 109-121.
- Francis, R. and Waterston, R. H. (1991). Muscle cell attachment in *Caenorhabditis elegans*. *J. Cell Biol.* **114**, 465-479.
- Frohman, M. A. (1993). Rapid amplification of complementary DNA ends for generation of full-length complementary DNAs: thermal RACE. *Methods Enzymol.* **218**, 340-356.
- Grant, K., Hanna-Rose, W. and Han, M. (2000). sem-4 promotes vulval cell-fate determination in *Caenorhabditis elegans* through regulation of lin-39 Hox. *Dev. Biol.* **224**, 496-506.
- Greenwald, I. (1997). Development of the vulva. In *Caenorhabditis elegans II* (ed. D. L. Riddle, T. Blumenthal, B. J. Meyer and J. R. Priess). Cold Spring Harbor, NY: Cold Spring Harbor Laboratory Press.
- Harris, J., Honigberg, L., Robinson, N. and Kenyon, C. (1996). Neuronal cell migration in *C. elegans*: regulation of Hox gene expression and cell position. *Development* **122**, 3117-3131.
- Henderson, K. D. and Andrew, D. J. (2000). Regulation and function of Scr, exd, and hth in the *Drosophila* salivary gland. *Dev. Biol.* **217**, 362-374.
- Hoier, E. F., Mohler, W. A., Kim, S. K. and Hajnal, A. (2000). The *Caenorhabditis elegans* APC-related gene apr-1 is required for epithelial cell migration and Hox gene expression. *Genes Dev.* **14**, 874-886.
- Hunter, C. P. and Kenyon, C. (1995). Specification of anteroposterior cell fates in *Caenorhabditis elegans* by *Drosophila* Hox proteins. *Nature* **377**, 229-232.
- Koh, K., Peyrot, S. M., Wood, C. G., Wagmaister, J. A., Maduro, M. F., Eisenmann, D. M. and Rothman, J. H. (2002). Cell fates and fusion in the *C. elegans* vulval primordium are regulated by the EGL-18 and ELT-6 GATA factors – apparent direct targets of the LIN-39 Hox protein. *Development* **129**, 5171-5180.
- Koh, K. and Rothman, J. H. (2001). ELT-5 and ELT-6 are required continuously to regulate epidermal seam cell differentiation and cell fusion in *C. elegans*. *Development* **128**, 2867-2880.
- Liu, J. and Fire, A. (2000). Overlapping roles of two Hox genes and the exd ortholog ceh-20 in diversification of the *C. elegans* postembryonic mesoderm. *Development* **127**, 5179-5190.
- Lu, X. and Horvitz, H. R. (1998). lin-35 and lin-53, two genes that antagonize a *C. elegans* Ras pathway, encode proteins similar to Rb and its binding protein RbAp48. *Cell* **95**, 981-991.
- Maconochie, M. K., Nonchev, S., Studer, M., Chan, S. K., Popperl, H., Sham, M. H., Mann, R. S. and Krumlauf, R. (1997). Cross-regulation in the mouse HoxB complex: the expression of Hoxb2 in rhombomere 4 is regulated by Hoxb1. *Genes Dev.* **11**, 1885-1895.
- Maloof, J. N. and Kenyon, C. (1998). The Hox gene lin-39 is required during *C. elegans* vulval induction to select the outcome of Ras signaling. *Development* **125**, 181-190.
- Maloof, J. N., Whangbo, J., Harris, J. M., Jongeward, G. D. and Kenyon, C. (1999). A Wnt signaling pathway controls hox gene expression and neuroblast migration in *C. elegans*. *Development* **126**, 37-49.
- Mello, C. C., Kramer, J. M., Stinchcomb, D. and Ambros, V. (1991). Efficient gene transfer in *C. elegans*: extrachromosomal maintenance and integration of transforming sequences. *EMBO J.* **10**, 3959-3970.
- Mohler, W. A., Shemer, G., del Campo, J. J., Valansi, C., Opoku-Serebuoh, E., Scranton, V., Assaf, N., White, J. G. and Podbilewicz, B. (2002). The type I membrane protein EFF-1 is essential for developmental cell fusion. *Dev. Cell* **2**, 355-362.
- Mohler, W. A., Simske, J. S., Williams-Masson, E. M., Hardin, J. D. and White, J. G. (1998). Dynamics and ultrastructure of developmental cell fusions in the *Caenorhabditis elegans* hypodermis. *Curr. Biol.* **8**, 1087-1090.
- Passner, J. M., Ryoo, H. D., Shen, L., Mann, R. S. and Aggarwal, A. K. (1999). Structure of a DNA-bound Ultrabithorax-Extradenticle homeodomain complex. *Nature* **397**, 714-719.
- Peifer, M. and Wieschaus, E. (1990). Mutations in the *Drosophila* gene extradenticle affect the way specific homeo domain proteins regulate segmental identity. *Genes Dev.* **4**, 1209-1223.
- Piper, D. E., Batchelor, A. H., Chang, C. P., Cleary, M. L. and Wolberger, C. (1999). Structure of a HoxB1-Pbx1 heterodimer bound to DNA: role of the hexapeptide and a fourth homeodomain helix in complex formation. *Cell* **96**, 587-597.
- Popperl, H., Bienz, M., Studer, M., Chan, S. K., Aparicio, S., Brenner, S., Mann, R. S. and Krumlauf, R. (1995). Segmental expression of Hoxb-1 is controlled by a highly conserved autoregulatory loop dependent upon exd/pbx. *Cell* **81**, 1031-1042.
- Popperl, H., Rikhof, H., Chang, H., Haffter, P., Kimmel, C. B. and Moens, C. B. (2000). lazarus is a novel pbx gene that globally mediates hox gene function in zebrafish. *Mol. Cell* **6**, 255-267.
- Rieckhof, G. E., Casares, F., Ryoo, H. D., Abu-Shaar, M. and Mann, R. S. (1997). Nuclear translocation of extradenticle requires homothorax, which encodes an extradenticle-related homeodomain protein. *Cell* **91**, 171-183.
- Saleh, M., Huang, H., Green, N. C. and Featherstone, M. S. (2000a). A conformational change in PBX1A is necessary for its nuclear localization. *Exp. Cell Res.* **260**, 105-115.
- Saleh, M., Rambaldi, I., Yang, X. J. and Featherstone, M. S. (2000b). Cell signaling switches HOX-PBX complexes from repressors to activators of transcription mediated by histone deacetylases and histone acetyltransferases. *Mol. Cell Biol.* **20**, 8623-8633.
- Salsler, S. J. and Kenyon, C. (1992). Activation of a *C. elegans* Antennapedia homologue in migrating cells controls their direction of migration. *Nature* **355**, 255-258.

- Shemer, G. and Podbilewicz, B.** (2002). LIN-39/Hox triggers cell division and represses EFF-1/fusogen-dependent vulval cell fusion. *Genes Dev.* **16**, 3136-3141.
- Shemer, G. and Podbilewicz, B.** (2003). The story of cell fusion: big lessons from little worms. *BioEssays* **25**, 672-682.
- Simmer, F., Tijsterman, M., Parrish, S., Koushika, S. P., Nonet, M. L., Fire, A., Ahringer, J. and Plasterk, R. H.** (2002). Loss of the putative RNA-directed RNA polymerase RRF-3 makes *C. elegans* hypersensitive to RNAi. *Curr. Biol.* **12**, 1317-1319.
- Solari, F. and Ahringer, J.** (2000). NURD-complex genes antagonise Ras-induced vulval development in *Caenorhabditis elegans*. *Curr. Biol.* **10**, 223-226.
- Sternberg, P. W. and Han, M.** (1998). Genetics of RAS signaling in *C. elegans*. *Trends Genet.* **14**, 466-472.
- Sternberg, P. W. and Horvitz, H. R.** (1986). Pattern formation during vulval development in *C. elegans*. *Cell* **44**, 761-772.
- Stoyanov, C. N., Fleischmann, M., Suzuki, Y., Tapparel, N., Gautron, F., Streit, A., Wood, W. B. and Muller, F.** (2003). Expression of the *C. elegans* labial orthologue *ceh-13* during male tail morphogenesis. *Dev. Biol.* **259**, 137-149.
- Streit, A., Kohler, R., Marty, T., Belfiore, M., Takacs-Vellai, K., Vigano, M. A., Schnabel, R., Affolter, M. and Muller, F.** (2002). Conserved regulation of the *Caenorhabditis elegans* labial/Hox1 gene *ceh-13*. *Dev. Biol.* **242**, 96-108.
- Studer, M., Gavalas, A., Marshall, H., Ariza-McNaughton, L., Rijli, F. M., Chambon, P. and Krumlauf, R.** (1998). Genetic interactions between Hoxa1 and Hoxb1 reveal new roles in regulation of early hindbrain patterning. *Development* **125**, 1025-1036.
- Sulston, J. and Hodgkin, J.** (1988). Methods. In *The Nematode Caenorhabditis elegans* (ed. W. B. Wood), pp. 587-605. Cold Spring Harbor, NY: Cold Spring Harbor Laboratory Press.
- Sulston, J. E. and Horvitz, H. R.** (1977). Post-embryonic cell lineages of the nematode, *Caenorhabditis elegans*. *Dev. Biol.* **56**, 110-156.
- Sym, M., Robinson, N. and Kenyon, C.** (1999). MIG-13 positions migrating cells along the anteroposterior body axis of *C. elegans*. *Cell* **98**, 25-36.
- Tan, P. B., Lackner, M. R. and Kim, S. K.** (1998). MAP kinase signaling specificity mediated by the LIN-1 Ets/LIN-31 WH transcription factor complex during *C. elegans* vulval induction. *Cell* **93**, 569-580.
- Van Auken, K., Weaver, D., Robertson, B., Sundaram, M., Saldi, T., Edgar, L., Elling, U., Lee, M., Boese, Q. and Wood, W. B.** (2002). Roles of the Homothorax/Meis/Prep homolog UNC-62 and the Exd/Pbx homologs CEH-20 and CEH-40 in *C. elegans* embryogenesis. *Development* **129**, 5255-5268.
- van Dijk, M. A. and Murre, C.** (1994). extradenticle raises the DNA binding specificity of homeotic selector gene products. *Cell* **78**, 617-624.
- Wang, B. B., Muller-Immergluck, M. M., Austin, J., Robinson, N. T., Chisholm, A. and Kenyon, C.** (1993). A homeotic gene cluster patterns the anteroposterior body axis of *C. elegans*. *Cell* **74**, 29-42.
- Wang, M. and Sternberg, P. W.** (2001). Pattern formation during *C. elegans* vulval induction. *Curr. Top. Dev. Biol.* **51**, 189-220.
- Waskiewicz, A. J., Rikhof, H. A., Hernandez, R. E. and Moens, C. B.** (2001). Zebrafish Meis functions to stabilize Pbx proteins and regulate hindbrain patterning. *Development* **128**, 4139-4151.
- Waskiewicz, A. J., Rikhof, H. A. and Moens, C. B.** (2002). Eliminating zebrafish pbx proteins reveals a hindbrain ground state. *Dev. Cell* **3**, 723-733.
- Whangbo, J. and Kenyon, C.** (1999). A Wnt signaling system that specifies two patterns of cell migration in *C. elegans*. *Mol. Cell* **4**, 851-858.
- Williams, B. D., Schrank, B., Huynh, C., Shownkeen, R. and Waterston, R. H.** (1992). A genetic mapping system in *Caenorhabditis elegans* based on polymorphic sequence-tagged sites. *Genetics* **131**, 609-624.
- Yao, L. C., Liaw, G. J., Pai, C. Y. and Sun, Y. H.** (1999). A common mechanism for antenna-to-leg transformation in *Drosophila*: suppression of homothorax transcription by four HOM-C genes. *Dev. Biol.* **211**, 268-276.
- Zhang, H., Azevedo, R. B., Lints, R., Doyle, C., Teng, Y., Haber, D. and Emmons, S. W.** (2003). Global regulation of Hox gene expression in *C. elegans* by a SAM domain protein. *Dev. Cell* **4**, 903-915.